Deep-Sea Research I 56 (2009) 212–231

Contents lists available at ScienceDirect

Deep-Sea Research I

journal homepage: www.elsevier.com/locate/dsri

Zooplankton distribution and cross-shelf transfer of carbon in an area of complex mesoscale circulation in the northern California Current

J.E. Keister [a,*], W.T. Peterson [b], S.D. Pierce [c]

[a] School of Oceanography, University of Washington, Box 357940, Seattle, WA 98195, USA
[b] National Oceanic and Atmospheric Administration, Newport, OR, USA
[c] College of Oceanic and Atmospheric Sciences, Oregon State University, Corvallis, OR, USA

ARTICLE INFO

Article history:
Received 19 January 2008
Received in revised form
5 September 2008
Accepted 8 September 2008
Available online 24 September 2008

Keywords:
Zooplankton distributions
Upwelling filaments
Mesoscale circulation
California Current
Carbon cycling

ABSTRACT

We conducted a research cruise in late summer (July–August) 2000 to study the effect of mesoscale circulation features on zooplankton distributions in the coastal upwelling ecosystem of the northern California Current. Our study area was in a region of complex coastline and bottom topography between Newport, Oregon (44.7°N), and Crescent City, California (41.9°N). Winds were generally strong and equatorward for >6 weeks prior to the cruise, resulting in the upwelling of cold, nutrient-rich water along the coast and an alongshore upwelling jet. In the northern part of the study area, the jet followed the bottom topography, creating a broad, retentive area nearshore over a submarine shelf bank (Heceta Bank, 44–44.4°N). In the south, a meander of the jet extended seaward off of Cape Blanco (42.8°N), resulting in the displacement of coastal water and the associated coastal taxa to >100 km off the continental shelf. Zooplankton biomass was high both over the submarine bank and offshore in the meander of the upwelling jet. We used velocities and standing stocks of plankton in the upper 100 m to estimate that 1×10^6 m^3 of water, containing an average zooplankton biomass of ~20 mg carbon m^{-3}, was transported seaward across the 2000-m isobath in the meandering jet each second. That flux equated to offshore transport of >900 metric tons of carbon each day, and $4–5\times10^4$ tons over the 6–8 week lifetime of the circulation feature. Thus, mesoscale circulation can create disparate regions in which zooplankton populations are retained over the shelf and biomass can accumulate or, alternatively, in which high biomass is advected offshore to the oligotrophic deep sea.

1. Introduction

Coastal upwelling brings nutrient-rich water to the sea surface and creates highly productive coastal ecosystems in which zooplankton thrive. However, advective transport during upwelling is a challenge that plankton must overcome to avoid local extinction. In relatively warm areas of the ocean, rapid growth and short generation times may offset advective losses (Escribano and Hidalgo, 2000). In the northern California Current (NCC), where the cold temperature of upwelled water leads to longer development times, diel or ontogenetic vertical migrations by zooplankton to exploit vertical current shears have been proposed as the most likely compensation mechanisms (Peterson, 1998). However, studies that have provided careful calculations of the potential impact of vertical migration on retention (e.g. Batchelder et al., 2002b; Peterson, 1998; Wroblewski, 1982) have done so in

* Corresponding author. Tel.: +1 206 543 7620.
E-mail address: jkeister@u.washington.edu (J.E. Keister).

0967-0637/$ - see front matter © 2008 Elsevier Ltd. All rights reserved.
doi:10.1016/j.dsr.2008.09.004

areas where classical Ekman upwelling cell circulation dominates. In areas of more complex three-dimensional (3-D) alongshore and cross-shelf circulation, migration patterns that are effective in controlling population losses in closed-cell circulation schemes may no longer work, and losses to the deep ocean may be large.

Both coastline and bottom topography have profound influences on circulation patterns. Examples include vortices found over submarine canyons and seamounts (e.g. Hickey, 1997; Torres et al., 2004), island wakes (Caldeira et al., 2005), and oceanic filaments generated near coastal promontories (Haidvogel et al., 1991). Such features influence biological distributions, resulting in advection and redistribution of organisms (Mackas and Coyle, 2005; Mackas and Yelland, 1999). In addition to creating advective features, topography–current interactions can also generate retentive areas where advection is low relative to surrounding areas. Examples of these are upwelling 'shadows' (Graham and Largier, 1997; Wing et al., 1998), re-circulation over submarine banks (Ashjian et al., 2001), and stationary eddies (Nishimoto and Washburn, 2002). In these areas, where local growth may keep pace with or exceed advective losses, biomass may be considerably elevated above surrounding areas, creating localized 'hot spots' important to population survival and the transfer of energy to upper trophic levels.

Several distinct regions of coastline and bottom topography occur in the NCC. Off northern and central Oregon (north of ~44.5°N), the coastline and bottom topography vary gradually alongshore. Between 43.8°N and 44.5°N, a large, shallow submarine bank (Heceta Bank) extends >100 km to sea. Farther to the south, Cape Blanco (42.8°N), Cape Mendocino (40°N), and Pt. Arena (39°N) are large coastal promontories that cause sharp deviations in the coastline. These topographic regions differ in the complexity of alongshore and cross-shelf circulation patterns that occur during summer upwelling. Coastal upwelling results in an alongshore, equatorward-flowing upwelling jet that develops through the upwelling season from a simple, alongshore current to a complex meandering current that can only maintain connection with the bathymetry in regions of relatively simple topography (Barth et al., 2005a; Gan and Allen, 2005). Where the jet is oriented along isobaths, it may act as a barrier to offshore transport (Castelao and Barth, 2005); where it deviates from the topography, it can create strong flow across isobaths. Off northern and central Oregon, the equatorward jet flows along isobaths, roughly parallel to the coastline throughout the upwelling season. The classic Ekman-driven two-dimensional (2-D) upwelling cell dominates the zonal circulation. However, when the upwelling jet encounters Heceta Bank, it deviates around the seaward margin of the bank, creating a wide area of upwelled water nearshore (Barth et al., 2005b; Gan and Allen, 2005), where flow is sluggish and re-circulation occurs (Castelao and Barth, 2005). The jet meanders strongly offshore at Cape Blanco (Barth et al., 2005b, 2000), causing strong zonal flows. At Cape Blanco and each of the more southern promontories, cold filaments of the upwelling jet frequently extend far to sea, creating deep, strong cross-isobath flow with velocities and volume transport that far exceed those in Ekman transport (Kosro and Huyer, 1986; Strub et al., 1991).

Evidence of the importance of mesoscale circulation patterns on the distribution of plankton in the NCC is accumulating from several studies of individual advective features, all of which have demonstrated offshore transport of coastal taxa and biomass (Barth et al., 2002; Haury, 1984; Hood et al., 1990; Huntley et al., 2000, 1995; Mackas et al., 1991). Less attention has been paid to the biological impact of retentive areas (though see Largier et al., 2006; Roughan et al., 2006), even though such areas are potentially important to population growth and larval survival. Nearshore, mesoscale circulation may serve as a mechanism of either advective loss or retention of coastal populations, whereas advective features, such as upwelling filaments that cross the shelf break, may cause high transport of coastal organisms to the deep sea.

In late July–early August 2000 (hereafter August 2000), we investigated the role of mesoscale circulation on distributions of mesozooplankton in a study area between Newport, Oregon (44.7°N), and Crescent City, California (41.9°N), 2–145 km from shore. Concurrently, a fishing vessel conducted upper-ocean trawls for nekton, near-surface zooplankton (Reese and Brodeur, 2006; Reese et al., 2005), and gelatinous zooplankton (Suchman and Brodeur, 2005), while a third vessel towed instrument packages to investigate the hydrography and circulation (Barth et al., 2005b), optical properties (Cowles, unpub. data), fish and zooplankton acoustic targets (Pierce et al., 2003; Ressler et al., 2005; Sutor et al., 2005), particle distributions (Zhou and Zhu, 2002), and marine mammals and seabirds (Ainley et al., 2005; Tynan et al., 2005). The studies were part of the US Global Ocean Ecosystems Dynamics Northeast Pacific Program (GLOBEC NEP) Mesoscale Processes study (Batchelder et al., 2002a).

In this paper, we use zooplankton collected with net tows and community analysis techniques to assess the relationship between circulation features and zooplankton community structure. Our goal is to describe the relationship between mesoscale circulation and patterns of coastal zooplankton taxa in our study area, examine differences in distributions among taxa, and use zooplankton distributions and concurrent velocity fields to estimate the impact of circulation features on the advection of biomass from nearshore to the deep sea.

2. Methods

2.1. Field collections

We used conductivity–temperature–depth (CTD) profiles, vertical plankton tows, and a Multiple-Opening-Closing-Nets-and-Environmental Sensing System (MOCNESS) to study the physical and biological patterns from the R.V. *New Horizon* between 28 July and 12 August 2000. Our study area was between Newport, Oregon (44.7°N), and Crescent City, California (42°N), 2–145 km from shore. Cruise reports and data can be accessed through http://globec.coas.oregonstate.edu/.

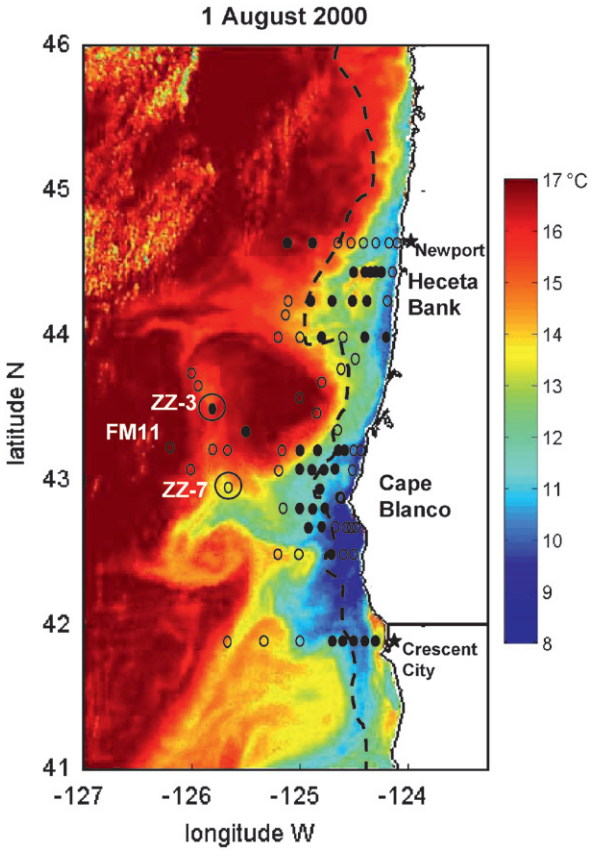

Fig. 1. Sea surface temperature image from the AVHRR on 1 August 2000 with locations of vertical net tows and CTD casts overlaid. Day (○) versus night (●) sampling is indicated by the symbols. The two stations analyzed for depth-distributions from MOCNESS sampling are labeled as ZZ-3 and ZZ-7 and circled and the location of the statistical outlier station, FM11, is shown. The seaward location of the 13.5 °C (yellow) isotherm roughly indicates the position of the core of the equatorward jet as defined in Barth et al. (2005b). The black dashed line is the 200-m isobath.

At each station (Fig. 1), zooplankton were collected with a 50-cm diameter, 202-μm mesh net towed vertically from near bottom (or 100 m depth in deep water) to the surface at a rate of 30 m min^{-1}. A TSK flowmeter was used to monitor the volume of water filtered. Samples were preserved in a 5% buffered formalin/seawater solution. In the laboratory, zooplankton samples were diluted to 5–10 times the settled volume and subsampled with a 1.1-ml stempel pipette. Two to four subsamples were counted for a total of typically 500–700 individuals per sample and 125–250 individuals of the dominant taxa. Copepods and euphausiids were identified by species and developmental stage. Other taxa were identified to genus when possible or larger taxonomic group otherwise. Euphausiid furcilia, chaetognaths, and pteropods (mainly *Limacina helicina*) were counted and their lengths were measured. The abundance of each taxonomic group (number of individuals m^{-3}) was calculated. Species diversity was calculated both as the total number of taxa at a location (species richness) and using H', the Shannon–Weiner diversity index (Macarthur and Macarthur, 1961; McCune and Grace, 2002):

$$H' = -\sum_{i}^{S} p_i \ln p_i$$

where p_i is the proportion of individuals from a sample unit belonging to species or taxon *i*. Biomass values (in mg carbon m^{-3}) were calculated by multiplying abundances with length–weight or stage-specific values found in the literature or generated in our laboratory (e.g. Chisholm and Roff, 1990; Peterson et al., 2002; Uye, 1982). With the exception of doliolids, gelatinous forms were included in abundance data, but not biomass calculations. Each taxon was examined for differences between daytime and nighttime densities using all samples collected. Those which are known to perform diel migration below the depth of our 100 m net casts (euphausiids older than furcilia stage III, shrimp larvae, crab larvae, chaetognaths, and fish larvae) were excluded. No others showed significant differences between day and night, even those that are able to migrate over >100 m ranges (e.g. the copepods *Calanus* spp., *Metridia pacifica*), so were retained in analyses. Other studies in our area have also shown little influence of diel migration on upper-100 m abundances (Peterson, 1972; Peterson and Keister, 2002; Shaw and Robinson, 1998).

In addition to vertical tows, a 1 m^2 mouth area MOCNESS equipped with 335 μm mesh nets was used to collect depth-stratified samples at several stations. Of those stations, two in the offshore areas of the upwelling filament (Fig. 1) were sorted for several dominant coastal and offshore copepod species to determine whether horizontal patterns seen in upper-100 m distributions were representative of those at depth.

At each location where zooplankton were collected, we also performed a CTD cast to 5 m off the bottom (maximum depth of 200 m in deep water) using a Sea-Bird SBE 911 plus CTD. At most stations, water samples were taken from multiple depths for analyses of chlorophyll and nutrient (NO_2, NO_3, PO_4) concentrations. Nutrients were analyzed by Oregon State University's chemical oceanography laboratory following the protocols of Gordon et al. (1994). Water for chlorophyll analysis was filtered onto Whatman GF/F filters. Chlorophyll-*a* was extracted with 90% acetone and analyzed using a Turner model 10 AU fluorometer. All maps of water and biological properties (Figs. 4, 5, 9, and 10) were generated by kriging the discrete data using spherical models with Surfer 8.03 software (Golden Software, Inc., 2002).

2.2. Satellite images

Sea surface temperature data from the Advanced Very High Resolution Radiometer (AVHRR) were captured with 1 km resolution and processed by Ocean Imaging of Solana Beach, California (www.oceani.com) for the US GLOBEC program. All are single-pass images, selected because they had the lowest cloud cover within the time period.

2.3. Velocity and transport estimates

Shipboard acoustic Doppler current profiler (ADCP) velocity data were collected from the R.V. *Wecoma*. We used an RD Instruments 153.6-kHz hull-mounted narrow-band profiler, with 8 m vertical bins and 2.5 min ensemble averaging. The shallowest data were from 17 m. Velocities were detided using the Erofeeva et al. (2003) tidal model. After removal of the barotropic tidal current, a baroclinic tidal signal may still be present. The baroclinic tide is challenging to estimate and highly variable in time and space. Semi-diurnal baroclinic tidal currents off Oregon can be as large as 0.10 m s^{-1} (Kurapov et al., 2003). For other ADCP processing details, see Barth et al. (2005b). Volume transports were estimated from profiles by integrating the observed velocities down to 100 m. Velocities shallower than 17-m were estimated by extending the 17-m value to the surface, i.e. a "slab" model. Biomass transports were estimated by multiplying interpolated vertical net biomass data by the volume transport, point by point approximately every 3 km along the chosen boundary (e.g. the 2000 m isobath) and normal to the local boundary orientation. See Fig. 3 caption for more detail.

2.4. Statistical analyses

We used non-parametric multivariate analyses to analyze zooplankton community structure (McCune and Grace, 2002). The original main "species" matrix had 82 stations $\times$ 64 taxa, with values in the matrix equal to the density (# m^{-3}) of each taxon at each station. Prior to analyses, data were $\mathrm{Log}_{10}(Y+0.01)+2$ transformed to normalize the variance while preserving distances among low values (McCune and Mefford, 2005). Rare taxa (those present in <3 samples) were removed to prevent them from strongly influencing results. The final matrix consisted of 82 stations $\times$ 52 taxa. All multivariate analyses were conducted in PC-ORD for Windows 5.05 (McCune and Mefford, 2005).

We sought groupings based on zooplankton community structure using agglomerative hierarchical cluster analysis with a Euclidean distance measure and Ward's Linkage Method (McCune and Grace, 2002). For presentation, the cluster dendogram is scaled both by Wishart's (1969) objective function and by percentage of information remaining. Wishart's objective function is a measure of information loss as clustering proceeds, and is calculated as the sum of the error sum of squares from the centroid of each group to the items in that group. No rigorous criteria exist for deciding how many cluster groupings to retain for discussion, but we used a multi-response permutation procedure (MRPP) (Mielke, 1984) and Indicator Species Analysis (ISA) (Dufrêne and Legendre, 1997) to help decide the optimal number of groupings. The *A*-statistic from MRPP (Field et al., 1982) assesses within-group homogeneity; thus, when calculated for groups identified by varying numbers of clusters, it can indicate the number of clusters at which within-group homogeneity peaks or plateaus—i.e. the number of clusters above which separation of the groups is not meaningful. From ISA (described below), a maximum total number of significant indicator species and a minimum overall averaged *p*-value (i.e. more significant results) help determine the optimal number of clusters.

A separate cluster analysis was performed on stations in 'environmental space.' The clustering method was identical to the zooplankton community clustering described above except that groupings were based only on the hydrographic variables (temperature, salinity, density) measured at 3, 20, and 50 m depths. Results of this cluster analysis identified groups of stations with similar hydrographic characteristics. A comparison of how stations grouped "hydrographically" versus in "taxonomic/community" structure helps elucidate the mechanisms of variability in community structure.

Following cluster analysis, ISA was used to investigate which taxa were driving the differences among the identified clusters. The indicator value (IV) for a species or taxon in a cluster group is calculated as the product of the relative abundance of the species in the group (the mean abundance in the group divided by the sum of the mean abundances in all groups) and the frequency of occurrence of the species in samples in the group. The statistical significance of each species IV was determined by a Monte Carlo method, in which sample units were randomly reassigned 1000 times to test if the IV was higher than expected by chance (Dufrêne and Legendre, 1997).

We used non-metric multi-dimensional scaling (NMDS) ordination using Sorensen's (Bray–Curtis) distance measure to examine similarities in zooplankton community composition among stations and to compare cluster groups to environmental (e.g. temperature, density, salinity, chlorophyll) gradients. NMDS was chosen for this analysis because it is considered one of the most robust ordination methods when dealing with zero–zero species density pairs (Field et al., 1982; Gray et al., 1988), which are common in our data. The final 'stress' (a measure of the goodness-of-fit between the data and the final ordination) was examined in relation to the ordination dimensionality to help choose the fewest dimensions necessary to adequately describe the data. Dimensionality was increased if the addition of an axis reduced the stress by >5, to a maximum of three dimensions, above which interpretation is prohibitively difficult. Stress values approaching or exceeding 20 are considered high; a value of zero indicates perfect monotonicity (McCune and Grace, 2002). The coefficient of determination (r^2) of each axis determines the proportion of the variation in the original distances that is represented by the axis. The Pearson correlation between each ordination axis and individual species and environmental parameters was used to measure the strength and direction (in relation to the axes) of relationships.

We correlated environmental variables with the NMDS ordination axes to examine which variables were important in the alignment of the zooplankton communities. The environmental variables we tested were hydrographic measurements at 3, 20, and 50 m depth (temperature, salinity, density) and chlorophyll and NO_3 measured from

water collected between 1 and 2 m depth (hereafter, 'surface').

3. Results

3.1. The physical setting

In the NCC, upwelling occurs seasonally in spring and summer. In 2000, the spring transition from poleward winds and downwelling, to equatorward winds and upwelling, occurred in mid-March. Prior to our cruise in August, upwelling winds had been exceptionally strong for >6 weeks (Barth et al., 2005b) resulting in cold, upwelled water all along the coast (Fig. 1). During our cruise, the meandering path of the jet caused expanded areas of cold, dense water over both the wide, shallow (<200 m) Heceta Bank, where the jet deviated westward to follow the bottom topography, and in a filament of water that extended seaward off of Cape Blanco (Fig. 1). A time series of satellite sea surface temperature (SST) images from AVHRR shows the development of upwelling over Heceta Bank area and the offshore filament (Fig. 2). Between 11 July and 23 July, the area of upwelled water over Heceta Bank expanded to the 200-m isobath, where it remained until early September. Off Cape Blanco, an offshore deviation of the jet had developed by 11 July, and by 23 July had turned anticyclonically to the northwest. Cold water was carried over the slope >100 km to sea, partially enclosing a warm pool to the north.

Measured ADCP velocities revealed a complex field of mesoscale circulation which included areas of retention and offshore advection (Fig. 3). Velocity vectors show strong flow, particularly along the offshore edge of the warm, anticyclonic water (~43.5°N 125.5°W) where it is nearly enclosed by the upwelling filament: depth-averaged (0–100 m) velocities reached $>50\,cm\,s^{-1}$ and 25 m velocities reached $>70\,cm^{-1}$ there (not shown). Strong westward flow occurred offshore of the northern and central edge of Heceta Bank (44.5°N 125.2°W), in the northwest-turning filament off Cape Blanco (42.9°N 125.3°N), and in the small filament present at the southwest corner of our study area (41.8°N 125.6°W). Velocities were very low over Heceta Bank, at the inshore edge of our two southernmost transects, and nearshore along 42.9°N. Velocities inshore of the 200-m isobath were nearly uniformly equatorward or shoreward north of Cape Blanco, but less uniform south of the Cape. The 250 m velocity field revealed a poleward undercurrent that hugged the seaward edge of the 200 m isobath (Fig. 3B).

Near-surface temperatures mapped using the CTD data (Fig. 4A) agree well with satellite SST although the features were not as well defined using discrete observations. Both the expanded area of upwelled water over Heceta Bank and off Cape Blanco were evident to >50 m depth (Fig. 4B). Near the surface of the filament (Fig. 4A and C), the gradients in temperature and density between the oceanic and upwelled water were stronger and occurred farther offshore than at depth (Fig. 4B and D), indicating deep mixing of the upwelled and oceanic water and weaker flow at depth. Station groups identified by hydrographic cluster analysis (using temperature, salinity, and density at three depths, (Fig. 4C) indicate that stations along the outer edge of the Heceta Bank complex, in the center of Heceta Bank, and off Cape Blanco from the nearshore out toward the edge of the filament (Group B) were hydrographically similar and differed from the offshore oceanic water (Group A). The region that hydrographic Group B occupied in the center of Heceta Bank had elevated temperatures and lower density values than surrounding stations indicating the influence of offshore water. That influence was not apparent at 50 m depth (Fig. 4B and D).

3.2. Biomass distribution

Zooplankton biomass was high in the cold, coastal water shoreward of the core of the upwelling jet (indicated in Fig. 1) all along the coast and offshore of Cape Blanco (Fig. 5). Biomass was low in the warm

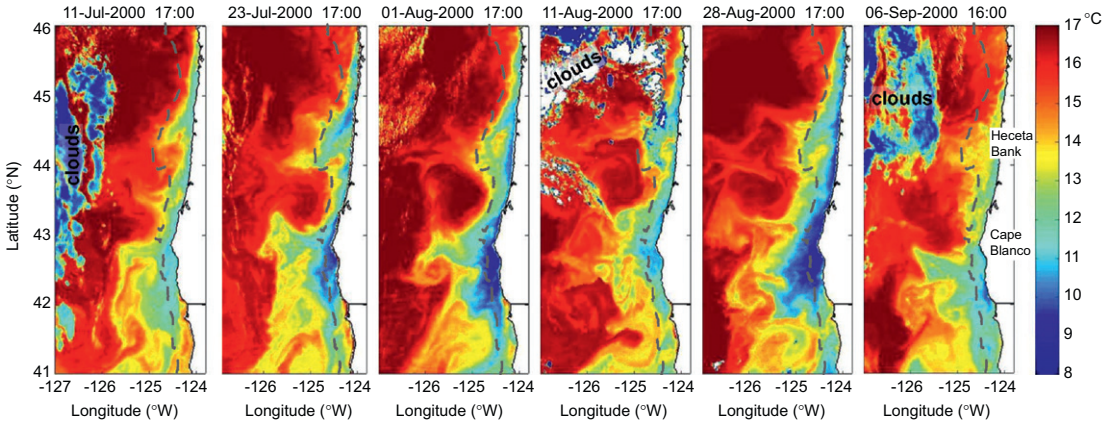

Fig. 2. Sea surface temperature images from the AVHRR showing the development of the upwelling system and the upwelling filament off of Cape Blanco labeled by local time and date. Images are the clearest single passes within 1–2 week intervals. Note that cloud masks are not applied. The 200-m isobath is shown as a dashed line.

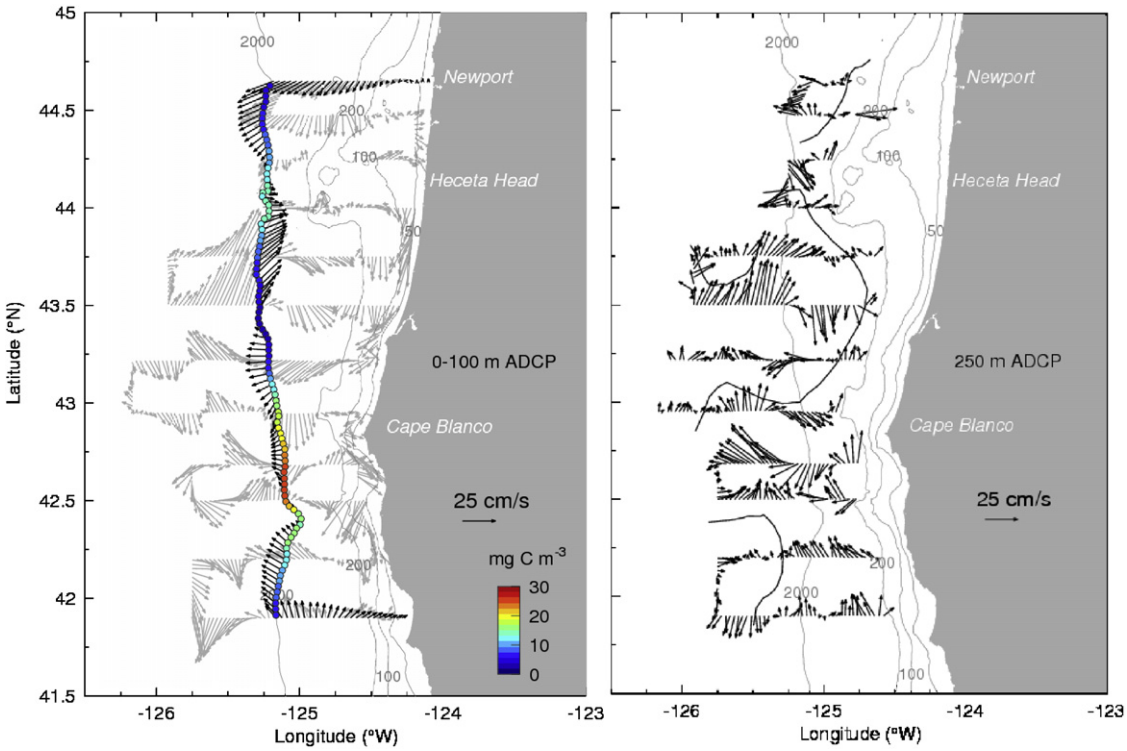

Fig. 3. Velocity vectors from the shipboard ADCP (left) depth-averaged over the upper 100 m and (right) at 250 m depth. The core of the upwelling jet, as defined in Barth et al. (2005b), is indicated by the solid line in the right panel. In the left panel, velocities interpolated along the 2000-m isobath and along the northern and southernmost transects are darker. Color circles indicate the zooplankton biomass, which was interpolated to each point location from the biomass data shown in Fig. 5. Isobaths are at 50, 100, 200, and 2000 m.

offshore water. Biomass was negatively correlated with near-surface temperature (Pearson's $r = -0.59$, $p < 0.008$), but was most strongly correlated with water density at 50 m depth (Fig. 6) indicating integrity of the biomass with water masses ($r = 0.77$, $p = 0.0001$ using log transformed data and a reduced N of 18 to account for autocorrelation) (Fig. 6). Zooplankton biomass was moderately correlated with surface chlorophyll ($r = 0.67$, $p = 0.002$). Chlorophyll was particularly high over Heceta Bank and south of the tip of Cape Blanco, but was also elevated in the offshore filament as compared to other areas of the deep ocean. Nitrate showed a strong relationship to the hydrography. Note the relationship between chlorophyll and nitrate (Fig. 5)—in areas of highest chlorophyll, especially over Heceta Bank and along the coast just south of the tip of Cape Blanco, nitrate is low compared to surrounding a regions, suggesting a draw-down of nutrients by the phytoplankton in those areas.

On average, copepods constituted 92% of the total biomass when strong migrators and medusae were excluded. Copepods were <70% of the total biomass at only seven stations—four were dominated by doliolids and salps whereas the other three had very high euphausiid egg or calyptopis abundances. When the migrators (late stage euphausiids, chaetognaths, etc.) but not medusae were included, copepods averaged 85% of the biomass.

3.3. Zooplankton communities

Cluster and ordination analyses revealed differences in zooplankton communities among stations. We chose to break the cluster dendogram at five cluster groups when guided by MRPP and ISA (Fig. 7). These cluster groups separated along the ordination axes (Fig. 8). The dimensionality of the ordination was determined by examining a plot of the stress versus number of axes to find the number of axes above which the reduction in stress was low. A 3-D ordination was selected based on the final moderate stress value of 14.2, compared to 20.2 for a 2-D solution and 11.1 for a 4-D solution. The moderate stress level indicates that the fine details of the ordination should not be relied upon (McCune and Grace, 2002). The final instability was <0.0001, indicating excellent stability of the solution. The ordination cumulatively represented 85.4% of the community variance. After rigid rotation of the axes to express the environmental variable with the highest correlation (water density at 50 m depth) such that it was expressed entirely along the 1st axis (i.e. zero correlation with Axes 2 and 3), Axis 1 accounted for most of the variance (61.2%) in zooplankton community composition. Axes 2 and 3 explained 10.6% and 13.7% of the remaining variance, respectively.

To identify potential outlier stations, we compared average community distances among stations. One of the 82 stations (FM11, 43.2°N, 126.2°W, Fig. 1) had an average

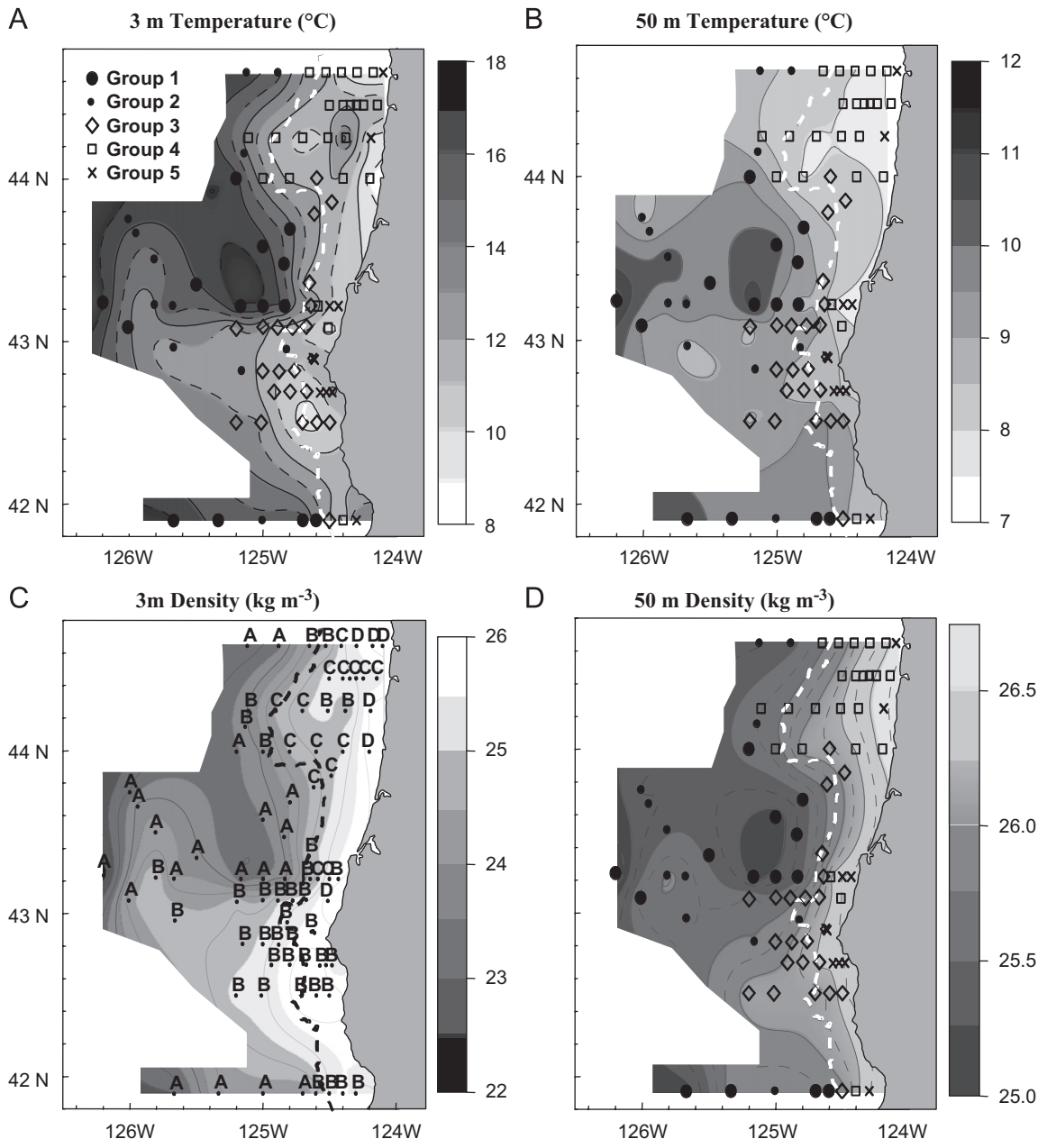

Fig. 4. Temperature and density at 3 and 50 m depths from CTD data. The 200-m isobath is shown as a dotted line. Symbols in A, B, and D represent zooplankton community cluster groupings identified by cluster analysis. Letters in C represent cluster groups defined by the hydrography rather than by the zooplankton taxonomic composition, where (A) 3 m Temperature (°C); (B) 50 m Temperature (°C); (C) 3 m Density (kg m^{-3}); (D) 50 m Density (kg m^{-3}).

Sorenson distance of 4.1 standard deviations from the grand mean. Station FM11 resided on an edge of the NMDS ordination plot, separated from other stations. However, its outlying position was not driven by unusual total abundances or distributions of any one, or few, taxa. This was the most offshore station we sampled, and highest surface ocean temperature and lowest salinity occurred there. Therefore, we determined that the station's position as an outlier most likely reflected its position at the extreme of the environmental gradients we measured, and hence brings valuable information to the analyses. Experimental removal of the station from analyses did not noticeably change the ordination of the remaining stations; therefore, station FM11 was retained in all multivariate analyses reported here.

Density, salinity, and temperature at all depths were strongly correlated with Axis 1 of the ordination (Table 1, Fig. 8). Of the environmental variables we measured, the water density at 50 m was most strongly related to the axis ($r = 0.87$) though near-surface and 20-m

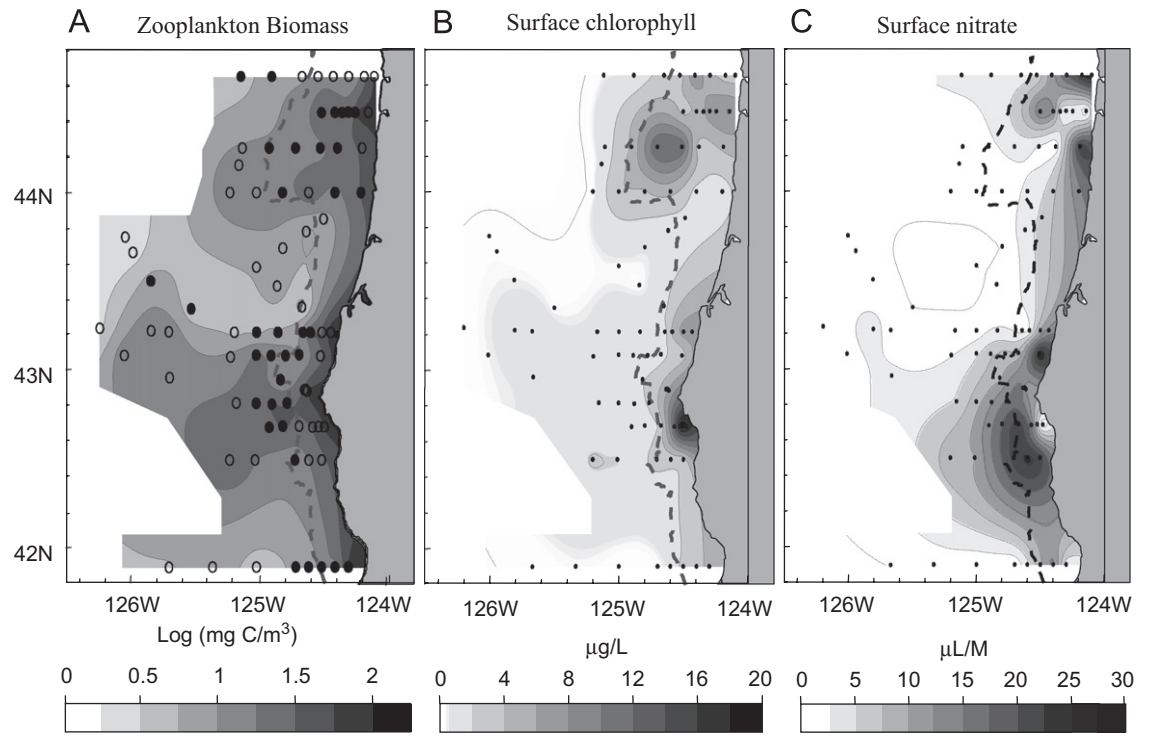

Fig. 5. (A) Zooplankton biomass integrated over the upper 100 m from vertical net tows. Strong migrators (see text) and medusae have been excluded. Symbols code for day (○) or night (●) sampling. (B) Total chlorophyll from near-surface bottle samples. (C) NO_3 from near-surface bottle samples. The 150-m isobath is the gray dashed line in each plot.

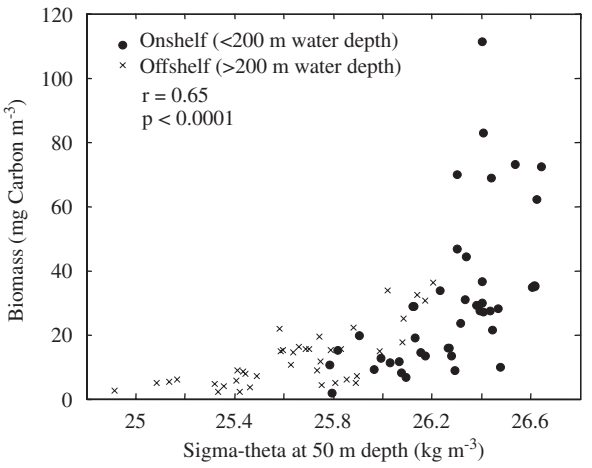

Fig. 6. Total zooplankton biomass, excluding strong migrators and medusae, integrated over the upper 100 m in relation to density at 50 m depth. The Pearson correlation and significance level are given. Data are coded by whether they were from on the continental shelf in <200 m water depth, or offshelf in >200 m water depth.

temperatures were also strongly negatively correlated ($r = -0.80$ and -0.82, respectively). Those hydrographic variables were more strongly correlated with Axis 1 than either longitude ($r = 0.74$), distance from shore ($r = -0.76$), or bottom depth ($r = -0.67$) indicating that the hydrographic variables were more important controls on zooplankton community composition than location relative to the shelf or shore. Latitude was very weakly correlated with Axis 1 ($r = 0.22$), but was the strongest variable correlated with Axis 3 ($r = -0.58$). Other than latitude, no variable correlated with either Axis 2 or Axis 3 with $R^2 > 0.2$.

Cluster groups were clearly associated with particular locations and hydrography (Fig. 4 symbols). Group 1 (●) was present only offshore where surface water was warm. Group 2 (•), which clustered closely with Group 1, occurred in slightly cooler water just off the shelf in the north, and in the offshore expression of the upwelling filament off Cape Blanco. Group 3 (◇) occupied the shelf region around the tip of Cape Blanco and extended off the shelf in the cold, dense filament. Group 4 (□) dominated the zooplankton community over the Heceta Bank complex although a few expressions of this community occurred nearshore farther south. Group 5 (×) was distinct compared to the other cold-water groups based on the level at which it grouped in the dendogram and its location in the ordinations. Group 5 occurred only very nearshore all along the coast.

Zooplankton community clusters showed strong hydrographic differences among cluster groups (Table 2), which are also revealed through the correlations between environmental variables and the ordination axes (Table 2, Fig. 8). In general, temperatures decreased and salinity and density increased across groups, with warmest temperatures, lowest salinities, and lowest density occurring in Group 1 and the opposite in Group 5. Locations where Groups 1 and 2 occurred were several degrees

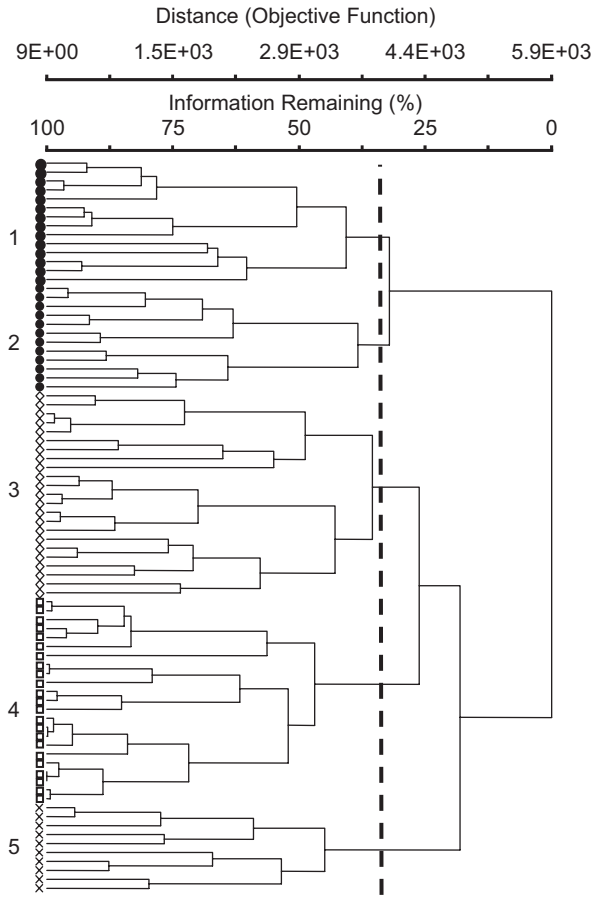

Fig. 7. Zooplankton community dendogram of stations clustered in species space. Symbols are the same as in Fig. 4. Cluster number is identified along the left.

warmer at 3 m depth than where other groups occurred. The hydrography where Groups 3 and 4 occurred (around Cape Blanco vs. over Heceta Bank) differed only slightly and is reflected in the lack of separation of the two groups along Axis 1. The groups separated along Axis 3 of the ordination (Fig. 8), indicating a stronger correlation with latitude than hydrography. Two warm-water, oceanic species, *Acartia danae* and *Calocalanus styliremis*, were found almost exclusively in Group 1 and were moderately negatively correlated with Axis 1.

Of the 52 taxa examined, 29 showed strong patterns in abundance along hydrographic variables and among cluster groups (Table 2, Figs. 9 and 10). Several of the most abundant species (e.g. *Pseudocalanus mimus*, *Acartia longiremis*, *Calanus marshallae*, and *Centropages abdominalis*) showed gradations in abundance from Group 5 through Group 1: abundances were highest in the nearshore cluster (Group 5), high over Heceta Bank (Group 4), and decreased steadily from the nearshore portion of the upwelling filament to the offshore tip, to the warm, deep ocean (Group 3 to Group 2 to Group 1). All of these taxa were strongly positively correlated with Axis 1 of the ordination (Table 3). Because Axis 1 represents low-to-high temperature and high-to-low salinity and density gradients, positive species correlations along that axis indicate increasing abundances from the warm, fresh offshore water to the cold, dense nearshore water. Several taxa (e.g. *Calanus pacificus*, *Clausocalanus arcuicornis*, and *Oncaea* spp.) showed the reverse pattern—they were most abundant in Group 1, least abundant or absent in Group 5, and negatively correlated with Axis 1.

We separate the study area into four dynamic biogeographic regions based on the zooplankton communities identified by the taxonomic cluster analysis: the very nearshore (Cluster Group 5), the most offshore (Groups 1 and 2), and the mid-shelf communities north (over Heceta Bank, Group 4) and south (off Cape Blanco, Group 3). The offshore, warm-water groups (Groups 1 and 2) had the highest number of taxa, highest Shannon's diversity indices, and highest number of significant indicator species (Table 2). The very nearshore (Group 5) and most offshore (Groups 1 and 2) communities were the most dissimilar. Several taxa were good indicators of those contrasting communities (Table 2), meaning that those taxa were found most consistently in highest abundances at the locations that made up the clusters. Strongest indicators of the offshore groups (Groups 1 and 2) were *Calocalanus styliremis*, several species of *Clausocalanus*, *Mesoscalanus tenuicornis*, *Oncaea* spp., *Paracalanus parvus*, and siphonophores. Strongest indicators of the very nearshore group (Group 5) were *Acartia hudsonica*, *Acartia longiremis*, *Calanus marshallae*, *Centropages abdominalis*, the cladocerans *Evadne* sp., and *Podon* sp., and gastropod and bivalve larvae.

Mid-shelf communities north (over Heceta Bank, Group 4) and south (off Cape Blanco, Group 3) separated from each other, but examination of the densities of animals in those clusters (Table 2) reveals few differences. Euphausiid eggs and nauplii were in uniquely high abundance over Heceta Bank, whereas euphausiid calyptopes and the small cyclopoid copepod, *Oithona similis*, were in highest abundance to the south. Those were the only taxa whose abundances were well correlated ($r>0.6$) with Axis 3 (Table 2, Fig. 10). Their correlations with Axis 3, along which Groups 3 and 4 separated, and their contrasting distributions in relation to Heceta Bank suggest that those taxa drove the separation of the two cluster groups. Other abundances between Groups 3 and 4 were similar.

Lastly, we examined the depth-distributions of several of the dominant copepods (*Calanus marshallae*, *Calanus pacificus*, *Acartia longiremis*, and *Pseudocalanus mimus*) at two offshore locations in the upwelling filament using MOCNESS collections to 350 m depth. Because the MOCNESS mesh size (335 μm) was too large to collect *Oithona similis*, we do not have vertical distribution data for that species. Depth-distributions varied by species (Fig. 11). The smaller, neritic copepods *Acartia longiremis* and *Pseudocalanus mimus* were restricted primarily to the upper 100 m, as has been noted at other locations in the NCC (Lamb and Peterson, 2005; Mackas and Galbraith, 2002), whereas the larger copepods, *Calanus marshallae* and *Calanus pacificus*, were distributed deeper. There were not apparent differences in vertical distributions due to the day/night sampling difference between the stations.

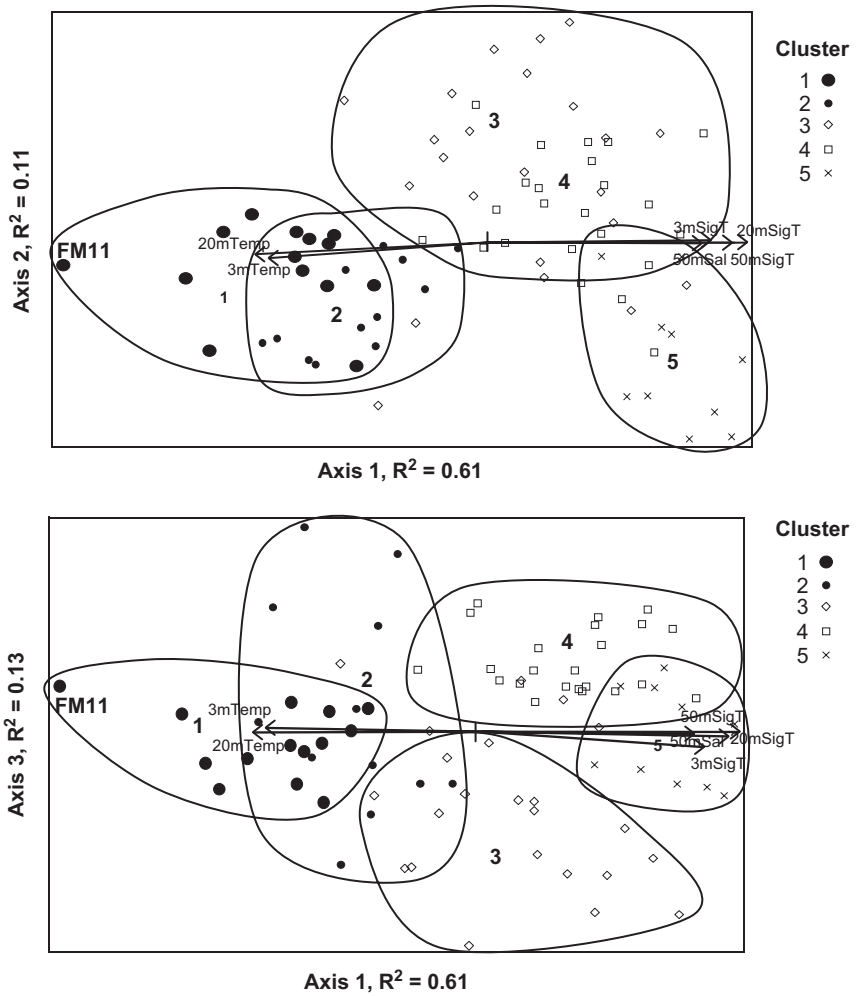

Fig. 8. Non-metric multidimensional scaling (NMS) ordination of stations based on species composition. Three-dimensional results shown as: Top, Axis 1 vs. Axis 2; Bottom, Axis 1 vs. Axis 3. Stations are coded by their cluster grouping as identified in cluster analyses (Fig. 7). The environmental gradients that correlated with the axes $R^2 > 0.6$ are shown; the direction of the correlation is indicated by arrows; the magnitudes of the correlations are given in Table 1.

4. Discussion

In late summer 2000, the meandering path of the equatorward upwelling jet created local areas of onshore retention and offshore advection. Where the jet deviated from the coastline to flow around Heceta Bank, it left an inshore area where current velocities were low and thus retention times were high. South of Heceta Bank, AVHRR images (Fig. 2) indicate that a meander of the jet developed off of Cape Blanco, extended >100 km offshore and broke down over an approximately 8-week period. Seaward ADCP velocities were high in the filament, indicating large offshore transport of water to the deep sea.

The effects of the hydrography on zooplankton distributions can easily be seen: zooplankton biomass was high where cold surface water was present nearshore, over the wide Heceta Bank area, and in the cool water advected offshore in the upwelling filament, but was low where surface waters were warm. The warm-water, oceanic taxa, which are commonly found throughout the area during winter (Keister and Peterson, 2003), were held offshore by the upwelling system in late summer. These taxa include the copepods *Clausocalanus* spp., *Paracalanus parvus*, and *Calanus pacificus*—they were in high numbers only well offshore and in the warm eddy off Cape Blanco (Fig. 9). In contrast, the cold-water taxa, which are the typical nearshore dominants during summer upwelling (Keister and Peterson, 2003), were abundant on the shelf, in the retentive area over Heceta Bank, and offshore in the advective filament off Cape Blanco. The patterns in zooplankton distributions seen result both from species affinities for different water masses (i.e. cold, upwelled water versus warm, oceanic water masses) and from the circulation patterns, which are indicated by horizontal gradients in density, salinity, and temperature.

4.1. Heceta Bank retentive area

Heceta Bank is known as a 'hot spot' where high standing stocks of chlorophyll, nekton, and upper trophic

Table 1
Pearson correlations between environmental variables and NMS ordination axes

	Axis 1		Axis 2		Axis 3	
	r	r^2	r	r^2	r	r^2
Latitude	0.22	0.05	−0.09	0.01	−0.58	0.33
Longitude	0.74	0.55	−0.21	0.04	−0.10	0.01
Depth	−0.67	0.45	0.29	0.08	0.09	0.01
Distance	−0.76	0.58	0.17	0.03	−0.15	0.02
On/off code	0.75	0.56	−0.14	0.02	−0.22	0.05
D/N code	−0.11	0.01	0.33	0.11	−0.01	0.00
3 m temperature	−0.80	0.64	0.21	0.05	−0.11	0.01
3 m salinity	0.70	0.50	0.07	0.01	0.30	0.09
3 m σ_θ	0.81	0.65	−0.08	0.01	0.22	0.05
20 m temperature	−0.82	0.67	0.18	0.03	0.05	0.00
20 m salinity	0.75	0.56	0.13	0.02	0.24	0.06
20 m σ_θ	0.85	0.72	−0.02	0.00	0.12	0.02
50 m temperature	−0.75	0.56	0.06	0.00	0.40	0.16
50 m salinity	0.79	0.62	0.04	0.00	0.09	0.01
50 m σ_θ	0.87	0.76	0.01	0.00	0.00	0.00
1 m Chl*a*	0.58	0.33	0.13	0.02	−0.09	0.01

D/N code is time of day, coded as day or night. On/off code is station depth coded as >200 or <200 m. Distance is distance from shore.

levels occur (e.g. Ainley et al., 2005; Reese and Brodeur, 2006; Ressler et al., 2005; Tynan et al., 2005). Low velocities over the bank have been noted in several previous studies (Barth et al., 2005a; Castelao and Barth, 2005; Kosro, 2005). Modeling and observations during a 2001 study of Heceta Bank indicated that low velocities over the bank result from the offshore movement of the upwelling jet where the shelf widens, leaving a lee inshore of the jet (Barth et al., 2005a; Gan and Allen, 2005; Kosro, 2005). In 2000, the water in this lee was retained long enough to warm (Barth et al., 2005a, b) and for primary production to draw down the ambient nutrients. Similar processes were noted in a 1995 study by van Geen et al. (2000), who reported biological draw-down of pCO_2 over Heceta Bank that did not occur south of Cape Blanco. The different advective regimes—active circulation in the south versus sluggish circulation over the bank—were implicated in the biological response.

The high abundance of euphausiid eggs on Heceta Bank reflects the location of spawning adults. Ressler et al. (2005) used acoustics and MOCNESS tows to study adult euphausiid distributions during this cruise. They report high abundances over Heceta Bank and directly offshore of Cape Blanco in cold chlorophyll-rich areas. Abundances elsewhere were very low. In euphausiid fecundity experiments (Gómez-Gutiérrez et al., 2007), only females collected from the Heceta Bank region produced large broods—females collected elsewhere produced small broods or did not spawn. From the distributions of spawning adults, eggs, and early life stages of euphausiids, it seems plausible that Heceta Bank was a primary spawning ground in August, from which larval euphausiids were advected south and offshore. Based on velocities measured where egg abundances were highest ($\leqslant 1$ km d^{-1} to the south, Fig. 3), eggs would not have been advected off the Bank before hatching into nauplii ~40 h after spawning. We estimate the path length between peak naupliar abundance and peak calyptopis abundance as ~200 km (Fig. 10), along which velocities of 17 ± 7 cm s^{-1} occurred; thus the journey would take ~8–20 days to complete. Because euphausiid nauplii develop to calyptopes in ~6–18 days (Feinberg et al., 2006), the distributions of the different euphausiid life stages support the hypothesis that the calyptopes found offshore were spawned over Heceta Bank. The distributions also indicate near-continuous spawning over the bank: only a small region between the stations where nauplii and calyptopes were abundant was devoid of larval euphausiids. If spawning was synchronized and infrequent, we likely would not have sampled all of the early life stages during the few (~6) days required to sample the study area. Furthermore, we returned to the transect at 44.3°N 1 week later (not shown) where we again sampled equally high abundances of euphausiid eggs indicating frequent high spawning over Heceta Bank that was not noted elsewhere.

The low velocities and high chlorophyll biomass over the Bank also provided suitable habitat for early life stages of other zooplankton. *Calanus marshallae* nauplii (the only copepod nauplii we quantitatively sampled) were abundant over the Bank area (Fig. 10). They were less abundant south of Cape Blanco and off the shelf, even south of the tip of Cape Blanco where chlorophyll was high (Figs. 5B and 10). The Heceta Bank region seems to be an example of an 'ocean triad' (Bakun, 1996) where zooplankton are concentrated (through high spawning), retained (by the slow circulation), and enriched (via upwelling and high chlorophyll biomass), thus creating the 'hot spot' of upper trophic activity (Reese and Brodeur, 2006).

4.2. Advective upwelling filament

In strong contrast to the retentive area over Heceta Bank, the seaward meander of the jet off Cape Blanco created a region of offshore, cross-isobath advection. Fastest seaward flow in the filament occurred along the northern margin, in the core of the cold water observed in the satellite image

Table 2
Characteristics of five station groupings identified by cluster analysis

Cluster group	1	2	3	4	5
Number of samples	14	12	23	23	10
Average number of taxa	24	18	15	14	16
Shannon's diversity index	3.13	2.87	2.62	2.57	2.73
Hydrographic characteristics					
Depth	1557 (1064)	1920 (1144)	599 (780)	182 (292)	62 (24)
Temperature at 3 m (°C)	16.1 (1.2)	14.6 (1.7)	11.7 (1.3)	11.6 (1.5)	11.2 (1.3)
Salinity at 3 m	32.4 (0.5)	32.5 (0.5)	33.1 (0.5)	32.9 (0.5)	33.6 (0.1)
σ_θ at 3 m	23.7 (0.6)	24.1 (0.7)	25.2 (0.5)	25 (0.6)	25.6 (0.3)
Temperature at 20 m (°C)	14 (1.7)	12.1 (1.6)	10.1 (1.1)	9.2 (0.7)	9.2 (0.6)
Salinity at 20 m	32.6 (0.3)	32.7 (0.4)	33.2 (0.4)	33.1 (0.4)	33.8 (0.1)
σ_θ at 20 m	24.3 (0.6)	24.8 (0.5)	25.6 (0.4)	25.6 (0.4)	26.1 (0.1)
Temperature at 50 m (°C)	9.8 (0.7)	9.3 (0.6)	9 (0.4)	8 (0.3)	8.2 (0.5)
Salinity at 50 m	33 (0.3)	33.1 (0.3)	33.6 (0.3)	33.6 (0.3)	33.9 (0.1)
σ_θ at 50 m	25.5 (0.3)	25.6 (0.2)	26 (0.2)	26.2 (0.3)	26.4 (0.1)
Chlorophyll-*a* at 1 m ($\mu g\,ml^{-1}$)	0.5 (0.4)	0.7 (0.5)	1.8 (1.2)	4.7 (3.1)	8.8 (5.9)
Zooplankton Biomass ($gC\,m^{-3}$)	6.7 (3.1)	11.8 (6.5)	17.9 (10.2)	25.9 (17.7)	63.2 (31.4)
Species abundances ($gC\,m^{-3}$)					
Copepods					
Acartia danae	3 (5)*	0 (1)	0 (0)	0 (0)	0 (0)
Acartia hudsonica	0 (0)	0 (0)	19 (37)	6 (12)	803 (1795)*
Acartia longiremis	88 (79)	133 (74)	412 (280)	480 (297)	1084 (706)*
Acartia tonsa	0 (1)	0 (0)	0 (1)	0 (1)	1 (4)
Calanus marshallae	5 (7)	8 (11)	79 (78)	91 (80)	232 (235)*
Calanus pacificus	4 (6)*	3 (4)	1 (3)	0 (1)	0 (0)
Centropages abdominalis	1 (2)	1 (2)	9 (15)	20 (27)	290 (495)*
Calocalanus styliremis	9 (10)*	0 (1)	0 (1)	1 (3)	0 (0)
Clausocalanus arcuicornis	17 (13)*	7 (16)	0 (1)	0 (0)	0 (0)
Clausocalanus parapergens	3 (5)*	0 (0)	1 (5)	0 (0)	0 (0)
Clausocalanus pergens	12 (17)*	1 (2)	4 (11)	1 (2)	0 (0)
Corycaeus spp.	0 (1)	4 (10)*	0 (0)	0 (0)	0 (0)
Ctenocalanus vanus	20 (15)*	7 (8)	16 (38)	1 (4)	3 (5)
Eucalanus spp.	1 (1)	1 (1)	0 (0)	0 (0)	0 (0)
Mesocalanus tenuicornis	13 (8)*	2 (2)	1 (3)	1 (4)	3 (6)
Metridia pacifica	13 (7)	16 (12)*	20 (15)	4 (5)	2 (8)
Oithona similis	679 (393)	742 (454)	835 (378)	404 (198)	1237 (690)*
Oncaea spp.	11 (8)*	2 (3)	3 (5)	0 (1)	0 (0)
Paracalanus parvus	159 (158)*	61 (50)	4 (8)	17 (20)	8 (10)
Pseudocalanus mimus	760 (664)	1157 (1063)	2319 (1083)	2412 (2091)	6827 (4073)*
Scolecithricella minor	2 (3)	0 (1)	4 (5)	3 (4)	2 (4)
Other taxa					
Euphausiid eggs	3 (3)	5 (10)	6 (12)	239 (285)*	125 (343)
Euphausiid nauplii	1 (2)	1 (2)	4 (12)	107 (166)*	129 (211)
Euphausiid calyptopes	109 (140)	147 (190)	11 (22)	35 (78)	174 (397)
Euphausiid furcilia	7 (9)	7 (6)*	4 (9)	2 (4)	48 (50)
Amphipods	0 (0)	0 (0)	1 (3)	0 (0)	6 (9)
Evadne sp.	0 (0)	0 (0)	1 (2)	3 (11)	242 (455)*
Podon sp.	0 (0)	0 (0)	1 (2)	0 (2)	242 (267)*
Gastropods	2 (5)	1 (2)	1 (5)	1 (2)	14 (22)*
Bivalves	0 (0)	0 (1.2)	2 (5)	2 (10)	288 (526)*
Polychaetes	1 (2)	1 (1)	0 (1)	3 (12)	66 (200)
Radiolarians	12 (13)	14 (13)*	3 (5)	0 (2)	0 (0)
Medusae	0 (0)	0 (0)	0 (0)	1 (3)	13 (34)
Larvaceans	130 (85)*	52 (69)	4 (13)	49 (67)	32 (27)
Doliolids	3 (7)	24 (50)*	0 (1)	0 (0)	0 (0)
Siphonophores	20 (18)*	16 (21)	0 (1)	0 (0)	0 (0)

Mean values with standard errors in brackets.
Only taxa that showed pattern across hydrographic variables or were significant indicators of a cluster group are shown. A * designates the cluster group for which a taxon's indicator value (IV) was significant.

west of the 2000 m isobath at ~42.7°N 125.3°W, and in the northwestward moving water in the northern extension of the filament. Weaker shoreward flow occurred along the southern margin of the filament. In the 'root' of the filament between the 200 and 2000 m isobaths, flow was not strongly directional and was generally weak.

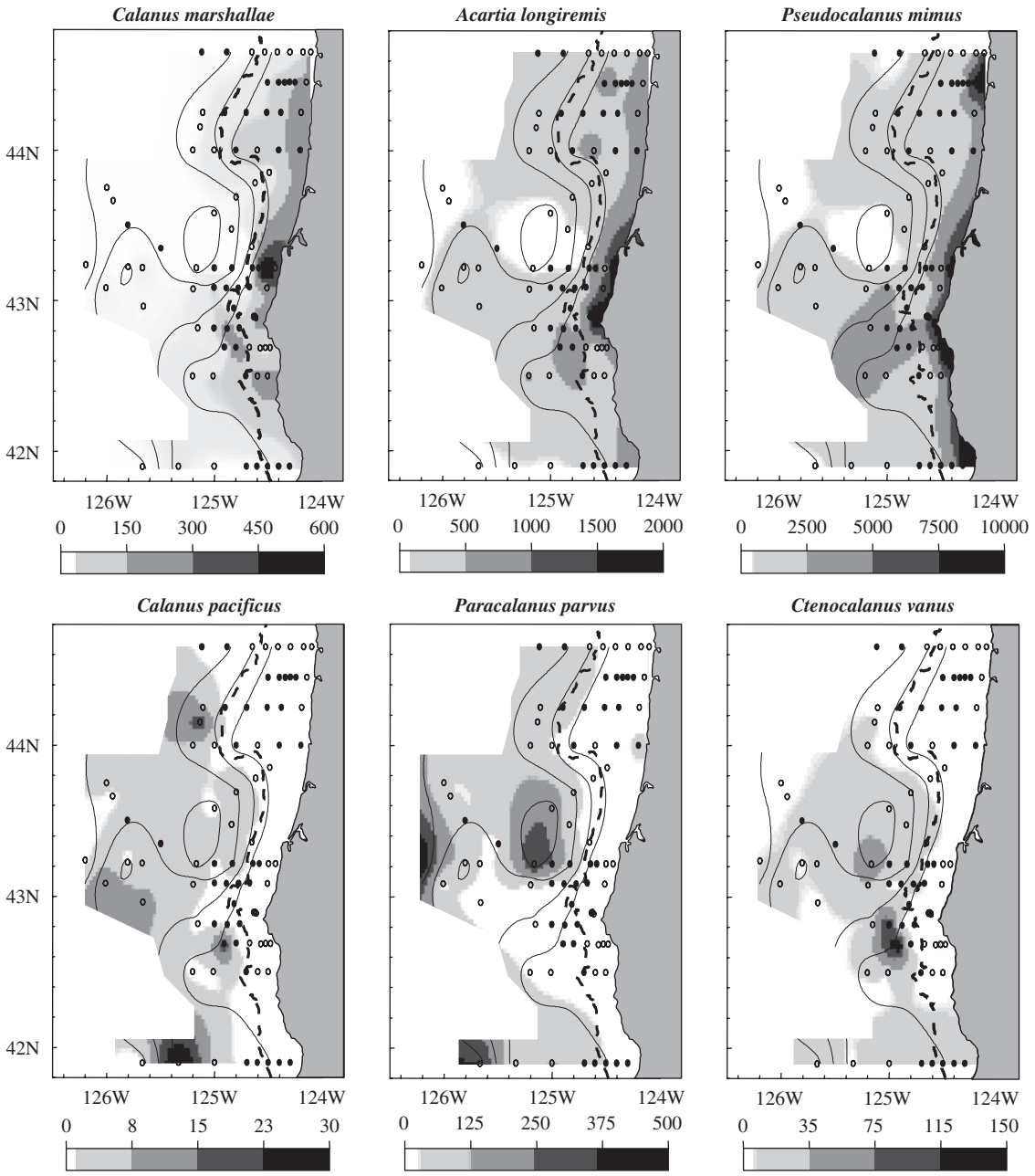

Fig. 9. Abundance of zooplankton which have strong correlations with Axis 1 of the NMDS ordination. Contours are from density at 50 m depth from CTD casts (Fig. 4) to show the relationship between the hydrography and distributions. Contour intervals are shown at each 0.25 from 25 to 26 kg m^{-3}. The 200-m isobath is shown as a dashed line.

Offshore advection of zooplankton within the filament is indicated by the distributions of several neritic taxa (Figs. 9 and 10), community composition (Fig. 4A) and the strong relationship between zooplankton biomass and water density (Fig. 6). All previous studies of the impact of mesoscale circulation features on biological distributions in the California Current have reported transport of coastal species large distances off the shelf. Haury (1984) described coastal copepod species in an eddy located >400 km to sea off Pt. Conception, California. Eddies surveyed offshore of Pt. Arena contained coastal zooplankton species (Huntley et al., 2000, 1995) and high biomass of chlorophyll (Barth et al., 2002) that had originated nearshore. Mackas et al. (1991) and Smith and Lane (1991) found high biomass of reproductively active coastal zooplankton in an upwelling filament >250 km off Pt. Arena, California. Studies in other eastern boundary current upwelling systems show the same effect

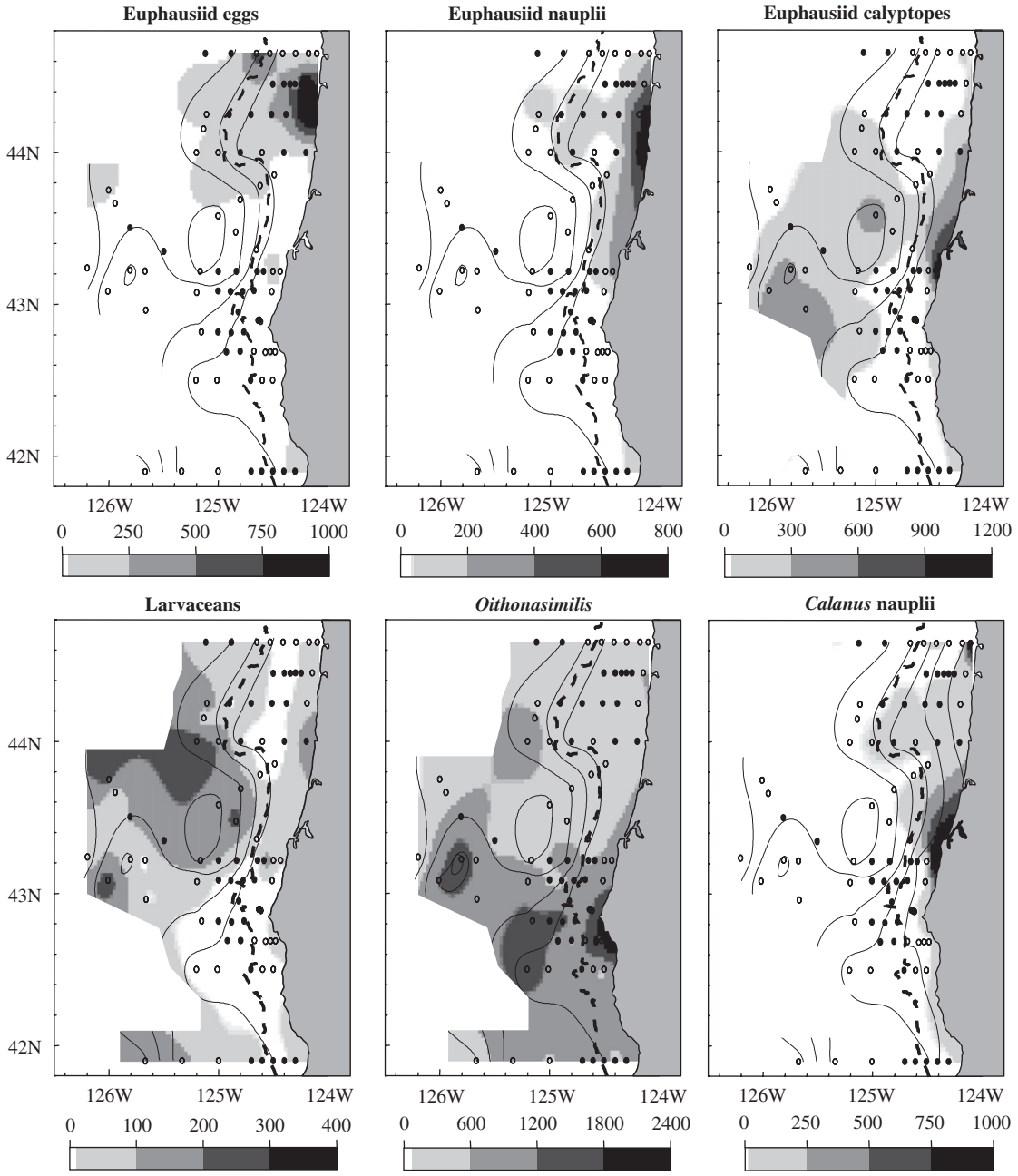

Fig. 10. Abundance of zooplankton which have strong correlations with Axis 2 or 3 of the NMDS ordination and *Calanus* nauplii. Contours are from density at 50 m depth from CTD casts (Fig. 4) to show the relationship between the hydrography and distributions. Contour intervals are shown at each 0.25 from 25 to 26 kg m^{-3}. The 200-m isobath is shown as a dashed line.

of upwelling filaments on species distributions (e.g. Escribano and Hidalgo, 2000; Hernández-León et al., 2002; Rodríguez et al., 1999).

As in Mackas et al. (1991), zooplankton biomass and species abundances were not uniformly distributed within the alongshore range of the filament—total biomass as well as abundance of several coastal taxa (e.g. *Acartia longiremis*, *Calanus marshallae*, *Scolecithricella minor*) were all higher in the slower moving southern 'core' of the filament than along the northern margin where seaward flows were fastest. In addition, our results appear to indicate a gradient in the effects of the offshore advection on neritic copepod distributions from the smallest taxa (*Oithona similis*, 1 μg C female^{-1}) (Fig. 10) through moderately sized taxa (e.g. *Pseudocalanus mimus*, 14 μg C female^{-1}, and *Acartia longiremis*, 6 μg C female^{-1}) (Fig. 9) to the largest taxa (*Calanus marshallae*, ~85 μg C female^{-1}) (Fig. 9). Smaller taxa were much more strongly associated with the bounds of the circulation patterns. For example, *O. similis* were found offshore in nearly as high abundance

Table 3
Pearson correlations between taxa and NMS ordination axes

	Axis 1		Axis 2		Axis 3	
	r	r^2	r	r^2	r	r^2
Acartia danae	**−0.55**	0.31	0.11	0.01	−0.02	0.00
Acartia hudsonica	**0.68**	0.46	0.39	0.15	0.20	0.04
Acartia longiremis	**0.73**	0.53	−0.02	0.00	0.16	0.03
Calanus marshallae	**0.83**	0.68	−0.09	0.01	0.21	0.04
Calanus pacificus	**−0.48**	0.23	0.27	0.07	0.17	0.03
Calocalanus styliremis	**−0.56**	0.32	0.12	0.01	0.02	0.00
Centropages abdominalis	**0.58**	0.34	0.20	0.04	0.01	0.00
Clausocalnus arcuicornis	**−0.73**	0.53	0.20	0.04	0.08	0.01
Clausocalnus parapergens	**−0.41**	0.17	0.03	0.00	0.09	0.01
Clausocalnus Pergens	**−0.47**	0.22	−0.05	0.00	0.06	0.00
Corycaeus spp.	**−0.29**	0.08	0.02	0.03	−0.05	0.00
Ctenocalanus vanus	**−0.70**	0.49	0.19	0.04	0.33	0.11
Mesocalanus tenuicornis	**−0.62**	0.39	0.21	0.05	0.18	0.03
Metridia pacifica	**−0.55**	0.30	−0.33	0.11	0.26	0.07
Oithona similis	0.15	0.02	0.29	0.08	**0.61**	0.38
Oncaea spp.	**−0.55**	0.31	0.08	0.01	0.33	0.11
Paracalanus parvus	**−0.55**	0.30	0.22	0.05	−0.44	0.19
Pseudocalanus mimus	**0.70**	0.49	0.06	0.00	0.35	0.12
Scolecithricella minor	−0.10	0.01	**−0.46**	0.21	0.19	0.04
Euphausiid eggs	0.19	0.04	−0.27	0.07	**−0.60**	0.36
Euphausiid nauplii	0.44	0.19	0.03	0.00	**−0.61**	0.37
Euphausiid furcilia I–III	−0.01	0.00	**0.59**	0.35	−0.01	0.00
Evadne sp.	**0.48**	0.23	0.33	0.11	−0.07	0.01
Podon sp.	**0.50**	0.25	0.48	0.23	0.12	0.02
Bivalve larvae	**0.42**	0.18	0.40	0.16	0.03	0.00
Radiolarians	**−0.70**	0.48	0.28	0.08	0.19	0.04
Gastropod larvae	0.05	0.00	**0.45**	0.20	−0.01	0.00
Larvaceans	−0.34	0.11	**0.59**	0.35	−0.44	0.20
Doliolids	**−0.51**	0.26	0.26	0.07	−0.33	0.11
Siphonophores	**−0.69**	0.48	0.19	0.04	0.09	0.01

The highest correlation with any axis is in bold. Only taxa that were significant indicators of a cluster group are shown.

as on the shelf, whereas, relative to nearshore abundances, *Calanus marshallae* were found offshore in very low abundances. Possibly, the larger taxa that were not found offshore in the upper layers of the filament exhibited behaviors that led them to migrate below the depth of our nets (>100 m) when they sensed increasing water temperatures or decreased chlorophyll offshore. Alternatively, because larger taxa may have higher food requirements (Vidal, 1980) or be subject to higher predation by visual predators (Luo et al., 1996), those taxa may have experienced higher mortality off the shelf than smaller taxa. This species-specific response to offshore advection has been noted in previous studies in this region (Peterson and Keister, 2002) and in eddies off British Columbia (Mackas and Galbraith, 2002). Because larger taxa are likely important prey items for visual predators, the mechanisms generating the patterns are of ecological interest.

The deeper vertical distribution of *Calanus marshallae* observed with the MOCNESS tows compared to the smaller coastal taxa (Fig. 11) suggests that the relative 'loss' of large taxa from the offshore filament may partly have been due to their migration below the depth of our vertical nets (max. depth of 100 m). Interestingly, *Calanus marshallae* were found almost exclusively in the deepest layers sampled whereas *C. pacificus* (75 μg C female^{-1}) were collected primarily from the upper 100 m. This contrast likely resulted from the different habitat preferences of the two species: *C. pacificus* is a warm-water species that usually inhabits the oligotrophic offshore waters whereas *C. marshallae* is a boreal, coastal species that thrives in cold, productive areas (Keister and Peterson, 2003). *C. marshallae*'s occurrence at depth may indicate that they descended to avoid the warm upper layers when carried off the shelf. However, the cues for such migration are not clear, and the low numbers even at depth (<20 m^{-3}) compared to nearshore prevent us from ruling out other explanations (i.e. predation or starvation) for their low numbers in the surface layer.

The relatively high abundances of *Oithona similis* in the Cape Blanco area compared to the Heceta Bank region is interesting (Fig. 10) and may indicate an affinity of that species to advective versus retentive regions. In the Benguela Current, *O. similis* is abundant in the highly advective Lüderitz upwelling region where most copepods cannot sustain high population densities (Huggett, 2008). Elevated production and biomass of *Oithona* in frontal regions has been reported (Castellani et al., 2007) theoretically because their ciliate prey are abundant there, but their relative absence from the Heceta Bank region remains unclear. Because *Oithona similis* is a numerically dominant species worldwide, the precise mechanisms allowing them to prosper in such advective regions warrants further study.

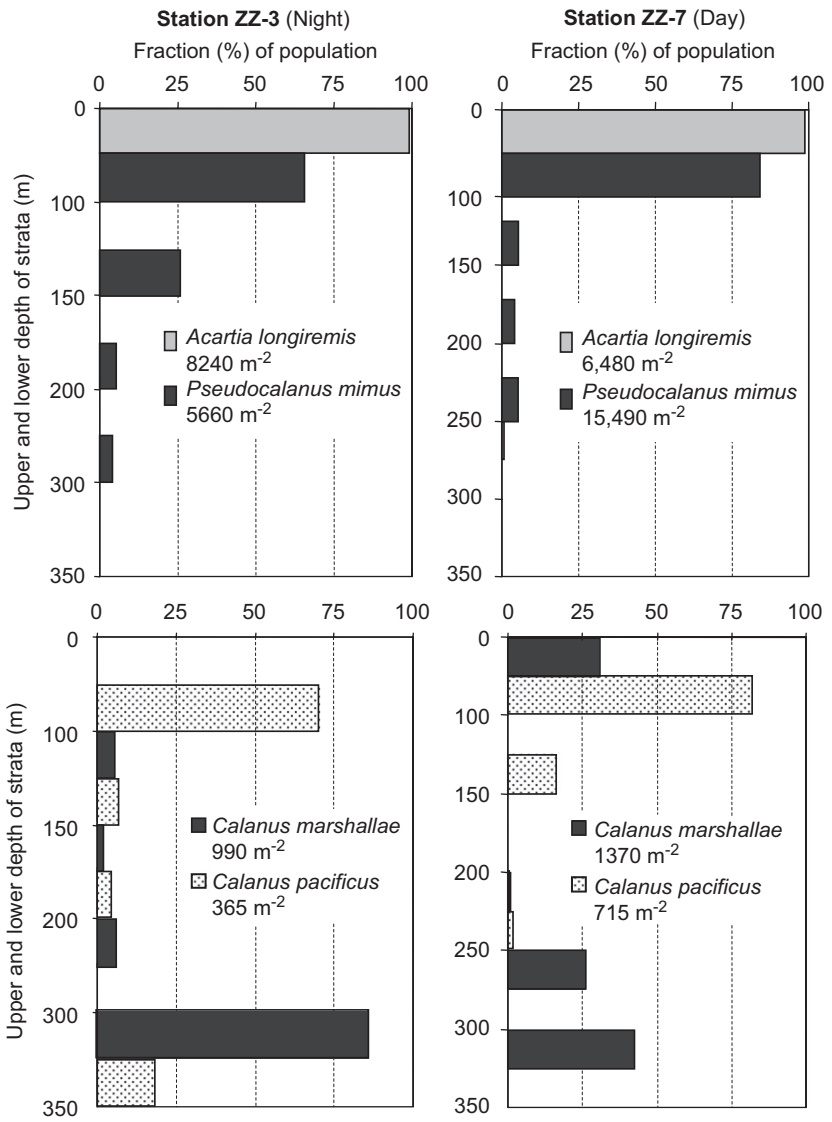

Fig. 11. Depth-distributions of copepods at stations ZZ-3 (left) and ZZ-7 (right) from MOCNESS tows expressed as the fraction of the species total upper 350 m abundance found in each depth interval. Station ZZ3 was sampled at night, ZZ7 during day. Total abundance m^{-2} in the upper 350 m is given for each species/station combination. The upper and lower depths of each sampling stratum are shown on the *y*-axes.

4.3. Transport estimates

Upwelling filaments can transport considerable volumes of water offshore, and often persist for several weeks through fluctuating wind conditions. We assessed the offshore transport of zooplankton biomass in the filament surveyed during this cruise using ADCP velocities and zooplankton biomass interpolated to points along the 2000-m isobath (black vectors and color circles in Fig. 3). For this purpose, we defined the alongshore range of the filament as 42.5–43.2°N based on satellite SST. That range includes the northern margin of the filament, where seaward velocities were high and zooplankton biomass was moderate, and the southern margin where velocities were weakly seaward or shoreward and biomass was very high.

Integrating upper 100 m velocities along the entire 2000-m isobath within the study area (41.9–44.6°N) resulted in a net offshore volume transport of 1.0 Sv ($1\,Sv = 10^6\,m^3\,s^{-1}$) and a flux of 1200 metric tons carbon per day in zooplankton biomass moving seaward. Transport across the isobath within the filament itself (42.5–43.2°N), though occupying only ~25% of the full latitudinal range, was about 50% of the total offshore transport (0.5 Sv seaward) and 75% of the biomass flux ($900\,tons\,C\,d^{-1}$). During the 6–8 week lifetime of the filament, $4–5 \times 10^4$ tons of C may have been delivered in the form of zooplankton biomass to the deep ocean. Even recognizing the difficulty in estimating fluxes from biomass estimates in a dynamic system and hence the errors they include (e.g. errors introduced by temporal changes in biomass and flow fields and by integrating

across discrete observations), the transport is significant and resulted in localized, elevated biomass offshore. Even >100 km off the shelf, biomass was 3–4 times higher within the filament than in surrounding oceanic water (Fig. 5).

After accounting for the flux of ~700 tons C d^{-1} that moved into the study area along our northernmost and southernmost transects (Fig. 3), and the 'instantaneous' standing stock of zooplankton inside the 2000 m isobath during the cruise (~3.2×10^4 tons C), a net seaward transport of ~2% of the biomass occurred per day in the upper 100 m. This is a conservative estimate because we have not accounted for velocity shear across the upper 17 m, or transport that occurred below 100 m depth, both potentially large fractions of the total. Considering that crustacean zooplankton (the dominant taxa in our samples) grow at ~0.1 d^{-1} (Peterson et al., 2002), advective losses were 15–20% of growth. This estimated flux is a larger portion of the inshore production than measured by Mackas and Yelland (1999) (<10%) in filaments off Vancouver Island, B.C., although their estimates included phytoplankton so are not directly comparable. In both regions, the offshore flux removed a small enough portion of the total that populations could have increased (depending on other losses such as predation) even while high advective losses occurred.

Studies of individual upwelling filaments in the Califonia Current System indicate that circulation dynamics within features differ spatially and temporally. Filaments can attain longer east–west spatial scales and higher volume transports than those measured here (Barth et al., 2000; Kosro and Huyer, 1986). So, because mesoscale circulation varies spatially and temporally (Keister and Strub, 2008) and wind-forcing can be stronger than it was in 2000 (Pierce et al., 2006), the offshore transport in filaments could easily be stronger in other years and at other locations.

Upwelling filaments transport coastal taxa to the deep sea in all four of the Eastern Boundary Current upwelling systems, but few quantitative measures of biomass fluxes have been reported to compare with the current study. In the Humboldt Current, Marin et al. (2003) used SeaWiFS data to estimate that ~1.6×10^3 metric tons of carbon per day was advected offshore in filaments, resulting in export of 5–12% of the coastal carbon production. That flux is on the order of that estimated here. Filaments in the Canary Current region are shallower (<100 m compared to >300 m) and lower velocity than those in the California and Humboldt Current systems, resulting in volume transports of 0.9–1.5 Sv compared to 1 to ⩾3 Sv in the California Current (Ramp et al., 1991; Barth et al., 2000; Leth and Shaffer 2001; Barton and Arístegui, 2004; Hernández-León et al., 2007; Sanchez, Relvas et al., 2008). Seaward carbon flux is likely to be comparatively low. Indeed, nutrients (Joint et al., 2001), chlorophyll, and copepod biomass (Halvorsen et al., 2001) reported within one Canary Current filament were all low compared to those measured in this study. Similar measurements in the Benguela Current have not yet been reported.

4.4. Transport pathways

Retention or return to the nearshore is ecologically necessary for maintenance of nearshore populations; thus, many coastal zooplankton have life history strategies that slow advective losses from the shelf to allow life cycle closure in upwelling ecosystems. These strategies can include ontogenetic and diel vertical migrations (Peterson, 1998) or high population growth rates (Escribano and Hidalgo, 2000). On Heceta Bank, low velocities indicated retention and small advective losses which may have allowed for high population growth and the high biomass we sampled there.

Whether plankton that are advected offshore in upwelling filaments can return to the shelf to complete their life cycle is unknown. Because velocities in the filament did not tend to strongly change direction with depth in the upper 300 m (not shown), migrations within the depths of most zooplankton's diel range (<100 m) would not substantially diminish their offshore transport or allow return to the shelf. However, one potential path of return from the offshore filament to nearshore is notable from hydrographic and zooplankton data collected during our study period: Barth et al. (2005b) noted that near-surface drifters did not closely track the deeper circulation. A drifter released over Heceta Bank traveled south alongshore, seaward to the northwest tip of the offshore filament, then completed an anticyclonic path when it crossed dynamic height contours and was entrained into the eastward moving jet on the southwestern edge of Heceta Bank at ~44°N 125.25°W (Barth et al., 2005b). Although the drifter did not return onto the shelf, it traveled >100 km shoreward from the deep ocean in <1 week. The disconnect between the surface and deep circulation indicates a potential way for zooplankton to return towards the shelf that was not available at depth.

Distributions of the small copepod *Oithona similis* (Fig. 10) seem to illustrate this pathway: abundances at the southern offshore edge of Heceta Bank were more similar to abundances in the northern offshore tip of the filament than to other locations within the bank region. It seems likely that the relatively high abundances at the edge of the Bank reflect a delivery of high numbers of individuals in near-surface circulation from offshore. Many of the dominant copepods in our study area reside just below the 10–20 m thick surface Ekman layer (Lamb and Peterson, 2005) and therefore would not have been able to exploit this return path. However, *O. similis* in our area typically occupy the upper 20 m Ekman layer (Lamb and Peterson, unpublished data) and so may have moved shoreward during a short-term wind reversal. Mackas and Galbraith (2002) noted that strong winds periodically move surface waters over eddies independently of the underlying geostrophic flow. Hence, taxa residing near-surface can be lost from geostrophic circulation features more easily than those beneath the Ekman layer.

It is not known whether the animals that do not return to the shelf contribute to secondary production in the offshore regions to which they have been moved. They may be subject to high predation over the continental slope and in the deep ocean where zooplanktivorous

euphausiids and fish reside. However, copepod egg production measurements made in upwelling filaments off California (Smith and Lane, 1991) and in the Canary Current (Hernández-León et al., 2002; Yebra et al., 2004) indicate that zooplankton may actively feed and reproduce in offshore expressions of features. In coastally generated eddies off Vancouver, Canada, coastal taxa are found offshore >15 months after separating from the shelf (Mackas and Galbraith, 2002). Hence, advected coastal populations may continue to contribute to offshore production for substantial lengths of time.

4.5. Trophic interactions

Biological relationships among the chlorophyll, zooplankton, and hydrography noted in this study corresponded to patterns exhibited by organisms in higher trophic levels. Reese and Brodeur (2006) identified Heceta Bank and the nearshore area around the tip of Cape Blanco as 'hot spots' of nekton biomass and species diversity. Abundances of juvenile coho and chinook salmon (Brodeur et al., 2004) and seabirds (Ainley et al., 2005) were also elevated in those regions. Many of the seabirds, particularly Shearwaters and Cassin's Auklets, were strongly related to frontal areas and locations of high chlorophyll biomass during this cruise. Humpback whales and harbor porpoises were strongly associated with areas of high chlorophyll biomass, whereas Dall's porpoises were found offshore around the edges of the filament (Tynan et al., 2005).

5. Conclusions

Mesoscale circulation features can advect huge volumes of coastal water offshore (Hormazabal et al., 2004; Kosro and Huyer, 1986; Mackas and Yelland, 1999). A single filament may advect as much water offshore as all of the Ekman transport along 1000 km of coastline (Kosro and Huyer, 1986). Several filaments simultaneously occur along the Oregon and California coast each summer. Their net offshore transport in coastal upwelling systems is clearly indicated by the dominance of neritic taxa within them (e.g. Haury, 1984; Mackas et al., 1991; Rodríguez et al., 1999). Here, we measured offshore transport in a meander of the upwelling jet as ~0.5 Sv, and a biomass flux of >900 tons of carbon per day in zooplankton alone. Coastal taxa, which are typically most abundant over the continental shelf (e.g. *Calanus marshallae*, *Acartia longiremis*, *Pseudocalanus mimus*), were abundant >100 km offshore in the filament, whereas warm-water, oceanic taxa were less abundant there.

Both the timing and intensity of mesoscale circulation (Keister and Strub, 2008) and peak nearshore zooplankton biomass (Peterson and Keister, 2002; Peterson and Miller, 1975) vary spatially and interannually in the NCC, so the biomass delivered to the deep sea, and hence the productivity of the ecosystem as a whole, are also likely to vary. Eastern boundary currents are highly productive in terms of primary and secondary production, so variability in the transfer of water and the associated planktonic communities between the shelf and deep ocean may have dramatic consequences for ecosystem dynamics and global carbon cycling, survival of oceanic zooplanktivores (e.g. Logerwell et al., 2001; Yen et al., 2006), and upper trophic level organisms (Palacios et al., 2006).

Acknowledgments

We thank T. Cowles and J. Barth, the captains and crew of the R/V *New Horizon* and R/V *Wecoma*, B. Hales for nutrient analysis, J. Fleischbein for CTD processing, and the many people who assisted with data collection at sea. Support for JEK was partially provided through Oregon State University's Cooperative Institute for Marine Resources Studies, award NA17RJ1362 from the National Oceanic and Atmospheric Administration (NOAA), US Department of Commerce (DOC) and through GLOBEC on NSF Grants NA67RJ0151, OCE-0435619, and OCE-0814698. SDP was supported through NSF Grant OCE-0435619. WTP was funded through NOAA Grant # NA860P0589. The statements, findings, conclusions, and recommendations are those of the authors and do not necessarily reflect the views of NOAA or the DOC. This paper is contribution # 606 from the US GLOBEC program, jointly funded by the National Science Foundation and NOAA.

References

Ainley, D.G., Spear, L.B., Tynan, C.T., Barth, J.A., Pierce, S.D., Ford, R.G., Cowles, T.J., 2005. Physical and biological variables affecting seabird distributions during the upwelling season of the northern California Current. Deep-Sea Research II 52, 123–143.

Ashjian, C.J., Davis, C.S., Gallager, S.M., Alatalo, P., 2001. Distribution of plankton, particles, and hydrographic features across Georges Bank described using the Video Plankton Recorder. Deep-Sea Research II 48, 245–282.

Bakun, A., 1996. Patterns in the Ocean: Ocean Processes and Marine Population Dynamics. California Sea Grant College System, La Jolla, CA, 323pp.

Barth, J.A., Pierce, S.D., Smith, R.L., 2000. A separating coastal upwelling jet at Cape Blanco, Oregon and its connection to the California Current System. Deep-Sea Research II 47, 783–810.

Barth, J.A., Cowles, T.J., Kosro, P.M., Shearman, R.K., Huyer, A., Smith, R.L., 2002. Injection of carbon from the shelf to offshore beneath the euphotic zone in the California Current. Journal of Geophysical Research 107.

Barth, J.A., Pierce, S.D., Castelao, R.M., 2005a. Time-dependent, wind-driven flow over a shallow midshelf submarine bank. Journal of Geophysical Research—Oceans 110.

Barth, J.A., Pierce, S.D., Cowles, T.J., 2005b. Mesoscale structure and its seasonal evolution in the northern California Current System. Deep-Sea Research II 52, 5–28.

Barton, E.D., Arístegui, J., 2004. The Canary Islands coastal transition zone—upwelling, eddies and filaments. Progress in Oceanography 62, 67–69.

Batchelder, H., Barth, J., Kosro, P., Strub, P., Brodeur, R., Peterson, W., Tynan, C., Ohman, M., Botsford, L., Powell, T., Schwing, F., Ainley, D., Mackas, D., Hickey, B., Ramp, S., 2002a. The GLOBEC Northeast Pacific California Current System Program. Oceanography 15, 36–47.

Batchelder, H.P., Edwards, C.A., Powell, T.M., 2002b. Individual-based models of copepod populations in coastal upwelling regions: implications of physiologically and environmentally influenced diel vertical migration on demographic success and nearshore retention. Progress in Oceanography 53, 307–333.

Brodeur, R.D., Fisher, J.P., Teel, D.J., Emmett, R.L., Casillas, E., Miller, T.W., 2004. Juvenile salmonid distribution, growth, condition, origin, and environmental and species associations in the Northern California Current. Fishery Bulletin 102, 25–46.

Caldeira, R.M.A., Marchesiello, P., Nezlin, N.P., DiGiacomo, P.M., McWilliams, J.C., 2005. Island wakes in the Southern California Bight. Journal of Geophysical Research—Oceans 110.

Castelao, R.M., Barth, J.A., 2005. Coastal ocean response to summer upwelling favorable winds in a region of alongshore bottom topography variations off Oregon. Journal of Geophysical Research—Oceans 110.

Castellani, C., Irigoien, X., Harris, R.P., Holliday, N.P., 2007. Regional and temporal variation of Oithona spp. biomass, stage structure and productivity in the Irminger Sea, North Atlantic. Journal of Plankton Research 29, 1051–1070.

Chisholm, L.A., Roff, J.C., 1990. Size–weight relationships and biomass of tropical neritic copepods off Kingston, Jamaica. Marine Biology 106, 71–77.

Dufrêne, M., Legendre, P., 1997. Species assemblages and indicator species: the need for a flexible asymmetrical approach. Ecological Monographs 67, 345–366.

Erofeeva, S.Y., Egbert, G.D., Kosro, P.M., 2003. Tidal currents on the central Oregon shelf models, data and assimilation. Journal of Geophysical Research 108.

Escribano, R., Hidalgo, P., 2000. Spatial distribution of copepods in the north of the Humboldt Current region off Chile during coastal upwelling. Journal of the Marine Biological Association of the United Kingdom 80, 283–290.

Feinberg, L.R., Shaw, C.T., Peterson, W.T., 2006. Larval development of *Euphausia pacifica* in the laboratory: variability in developmental pathways. Marine Ecology Progress Series 316, 127–137.

Field, J.G., Clarke, K.R., Warwick, R.M., 1982. A practical strategy for analysing multispecies distribution patterns. Marine Ecology Progress Series 8, 37–52.

Gan, J.P., Allen, J.S., 2005. Modeling upwelling circulation off the Oregon coast. Journal of Geophysical Research—Oceans 110.

Golden Software, Inc. 2002. Surfer, version 8.03. Golden Software, Inc., Golden, CO, USA.

Gómez-Gutiérrez, J., Feinberg, L.R., Shaw, C.T., Peterson, W.T., 2007. Interannual and geographical variability of the brood size of the euphasuiids Euphausia pacifica and Thysanoessa spinifera along the Oregon coast (1999–2004). Deep-Sea Research I 54, 145–2169.

Gordon, L.I., Jennings, J.J.C., Ross, A.A., Krest, J.M., 1994. A suggested protocol for continuous flow analysis of seawater nutrients (phosphate, nitrate, nitrite, and silicic acid) in the WOCE Hydrographic Program and the Joint Global Ocean Fluxes Study. Woods Hole, MA, WOCE Hydrograph. Prog., np.

Graham, W.M., Largier, J.L., 1997. Upwelling shadows as nearshore retention sites: the example of northern Monterey Bay. Continental Shelf Research 17, 509–532.

Gray, J.S., Aschan, M., Carr, M.R., Clarke, D.R., Green, R.H., Pearson, T.H., Rosenberg, R., Warwick, R.M., 1988. Analysis of community attributes of the benthic macrofauna of Frierfjord/Langesundfjord and in a mesocosm experiment. Marine Ecology Progress Series 46, 151–165.

Haidvogel, D.B., Beckmann, A., Hedstrom, K.S., 1991. Dynamical simulations of filament formation and evolution in the coastal transition zone. Journal of Geophysical Research 96, 15017–15040.

Halvorsen, E., Pedersen, O.P., Slagstad, D., Tande, K.S., Fileman, E.S., Batten, S.D., 2001. Microzooplankton and mesozooplankton in an upwelling filament off Galicia: modelling and sensitivity analysis of the linkages and their impact on the carbon dynamics. Progress in Oceanography 51, 499–513.

Haury, L.R., 1984. An offshore eddy in the California Current System. Part IV: Plankton distributions. Progress in Oceanography 13, 95–111.

Hernández-León, S., Almeida, C., Portillo-Hahnefeld, A., Gómez, M., Rodríguez, J.M., Arístegui, J., 2002. Zooplankton biomass and indices of feeding and metabolism in relation to an upwelling filament off northwest Africa. Journal of Marine Research 60, 327–346.

Hernández-León, S., Gómez, M., Arístegui, J., 2007. Mesozooplankton in the Canary Current System: the coastal–ocean transition zone. Progress in Oceanography 74, 397–421.

Hickey, B.M., 1997. The response of a steep-sides, narrow canyon to time variable wind forcing. Journal of Physical Oceanography 27, 697–726.

Hood, R.R., Abbott, M.R., Huyer, A., Kosro, P.M., 1990. Surface patterns in temperature, flow, phytoplankton biomass, and species composition in the coastal transition zone off northern California. Journal of Geophysical Research 95, 18081–18094.

Hormazabal, S., Shaffer, G., Leth, O., 2004. Coastal transition zone off Chile. Journal of Geophysical Research 109.

Huggett, J., 2008. Copepod biomass and production in the Southern Benguela—spatio-temporal patterns, links to pelagic fish and comparisons with other eastern boundary upwelling systems. Eastern Boundary Upwelling Ecosystems Symposium, Las Palmas de Gran Canaria, Spain.

Huntley, M.E., Zhou, M., Nordhausen, W., 1995. Mesoscale distribution of zooplankton in the California Current in late spring, observed by optical plankton counter. Journal of Marine Research 53, 647–674.

Huntley, M.E., González, A., Zhu, Y., Zhou, M., Irigoien, X., 2000. Zooplankton dynamics in a mesoscale eddy-jet system off California. Marine Ecology Progress Series 201, 165–178.

Joint, I., Rees, A.P., Woodward, E.M.S., 2001. Primary production and nutrient assimilation in the Iberian upwelling in August 1998. Progress in Oceanography 51, 303–320.

Keister, J.E., Peterson, W.T., 2003. Zonal and seasonal variations in zooplankton community structure off the central Oregon coast, 1998–2000. Progress in Oceanography 57, 341–361.

Keister, J.E., Strub, P.T., 2008. Spatial and interannual variability in mesoscale circulation in the northern California Current System. Journal of Geophysical Research.

Kosro, P.M., 2005. On the spatial structure of coastal circulation off Newport, Oregon, during spring and summer 2001 in a region of varying shelf width. Journal of Geophysical Research—Oceans 110.

Kosro, P.M., Huyer, A., 1986. CTD and velocity surveys of seaward jets off northern California, July 1981 and 1982. Journal of Geophysical Research 91, 7680–7690.

Kurapov, A.L., Egbert, G.D., Allen, J.S., Miller, R.N., 2003. M2 internal tide off Oregon: inferences from data assimilation. Journal of Physical Oceanography 33, 1733–1757.

Lamb, J.F., Peterson, W.T., 2005. Ecological zonation of zooplankton in the COAST study region off central Oregon in June and August 2001 with consideration of retention mechanisms. Journal of Geophysical Research 110.

Largier, J.L., Lawrence, C.A., Roughan, M., Kaplan, D.M., Dever, E.P., Dorman, C.E., Kudela, R.M., Bollens, S.M., Wilkerson, F.P., Dugdale, R.C., Botsford, L.W., Garfieldg, N., Cervantes, B.K., Koracin, D., 2006. WEST: a northern California study of the role of wind-driven transport in the productivity of coastal plankton communities. Deep-Sea Research II 53, 2833–2849.

Leth, O., Shaffer, G., 2001. A numerical study of the seasonal variability in the circulation off central Chile. Journal of Geophysical Research—Oceans 106, 22229–22248.

Logerwell, E.A., Lavaniegos, B.E., Smith, P.E., 2001. Spatially-explicit bioenergetics of Pacific sardine in the Southern California Bight: are mesoscale eddies areas of exceptional prerecruit production? Progress in Oceanography 49, 391–406.

Luo, J., Brandt, S.B., Klebasko, M.J., 1996. Virtual reality of planktivores: a fish's perspecive of prey size selection. Marine Ecology Progress Series 140, 271–283.

Macarthur, R.H., Macarthur, J.W., 1961. On bird species diversity. Ecology 42, 594–598.

Mackas, D.L., Coyle, K.O., 2005. Shelf-offshore exchange processes, and their effects on mesozooplankton biomass and community composition patterns in the northeast Pacific. Deep-Sea Research II 52, 707–725.

Mackas, D.L., Galbraith, M.D., 2002. Zooplankton distribution and dynamics in a North Pacific eddy of coastal origin: 1. Transport and loss of continental margin species. Journal of Oceanography 58, 725–738.

Mackas, D.L., Yelland, D.R., 1999. Horizontal flux of nutrients and plankton across and along the British Columbia continental margin. Deep-Sea Research II 46, 2941–2967.

Mackas, D.L., Washburn, L., Smith, S.L., 1991. Zooplankton community pattern associated with a California Current cold filament. Journal of Geophysical Research 96, 14781–14797.

Marin, V.C.H., Delgado, L.E., Luna-Jorquera, G., 2003. S-chlorophyll squirts at 30 degrees S off the Chilean coast (eastern South Pacific): feature-tracking analysis. Journal of Geophysical Research 108, 0.

McCune, B., Grace, J.B., 2002. Analysis of Ecological Communities. MjM Software Design, Gleneden Beach, OR, 300pp.

McCune, B., Mefford, M.J., 2005. PC-ORD, 5.0. MjM Software, Gleneden Beach, OR, USA.

Mielke, P.W.J., 1984. Meterological applications of permutation techniques based on distance functions. In: Krishnaiah, P.R., Sen, P.K. (Eds.), Handbook of Statistics: Nonparametric Methods, vol. 4. Elsevier Science Publishers, Amsterdam, pp. 813–830.

Nishimoto, M.M., Washburn, L., 2002. Patterns of coastal eddy circulation and abundance of pelagic juvenile fish in the Santa Barbara Channel, California, USA. Marine Ecology Progress Series 241, 183–199.

Palacios, D.M., Bograd, S.J., Foley, D.G., Schwing, F.B., 2006. Oceanographic characteristics of biological hot spots in the North Pacific: a remote sensing perspective. Deep-Sea Research II 53, 250–269.

Peterson, W.K., 1972. Distribution of pelagic Copepoda off the coasts of Washington and Oregon during 1961 and 1962. In: Pruter, A.T., Alverson, D.L. (Eds.), The Columbia River Estuary and Adjacent Ocean Waters. University of Washington Press, Seattle, pp. 313–343.

Peterson, W.T., 1998. Life cycle strategies of copepods in coastal upwelling zones. Journal of Marine Systems 15, 313–326.

Peterson, W.T., Keister, J.E., 2002. The effect of a large cape on distribution patterns of coastal and oceanic copepods off Oregon and northern California during the 1998/1999 El Niño/La Niña. Progress in Oceanography 53, 389–411.

Peterson, W.T., Miller, C.B., 1975. Year-to-year variations in the planktology of the Oregon upwelling zone. Fishery Bulletin 73, 642–653.

Peterson, W.T., Gómez-Gutiérrez, J., Morgan, C.A., 2002. Cross-shelf variation in calanoid copepod production during summer 1996 off the Oregon coast, USA. Marine Biology 141, 353–365.

Pierce, S.D., Barth, J.A., Peterson, W.T., Cowles, T.J., 2003. Bioacoustic surveys in the northern California Current System: zooplankton retention mechanisms. EOS Transactions American Geophysical Union 84, Abstract OS21-B23.

Pierce, S.D., Barth, J.A., Thomas, R.E., Fleischer, G.W., 2006. Anomalously warm July 2005 in the northern California Current: historical context and the significance of cumulative wind stress. Geophysical Research Letters 33.

Ramp, S.R., Jessen, P.F., Brink, K.H., Niiler, P.P., Daggett, F.L., Best, J.S., 1991. The physical structure of cold filaments near Point Arena, California, during June 1987. Journal of Geophysical Research 96, 14859–14883.

Reese, D.C., Brodeur, R.D., 2006. Identifying and characterizing biological hotspots in the northern California Current. Deep-Sea Research II 53, 291–314.

Reese, D.C., Miller, T.W., Brodeur, R.D., 2005. Community structure of near-surface zooplankton in the northern California Current in relation to oceanographic conditions. Deep-Sea Research II 52, 29–50.

Ressler, P.H., Brodeur, R.D., Peterson, W.T., Pierce, S.D., Vance, P.M., Rostad, A., Barth, J.A., 2005. The spatial distribution of euphausiid aggregations in the Northern California Current during August 2000. Deep-Sea Research II 52, 89–108.

Rodríguez, J.M., Hernández-León, S., Barton, E.D., 1999. Mesoscale distribution of fish larvae in relation to an upwelling filament off Northwest Africa. Deep-Sea Research I 46, 1969–1984.

Roughan, M., Garfield, N., Largier, J., Dever, E., Dorman, C., Peterson, D., Dorman, J., 2006. Transport and retention in an upwelling region: The role of across-shelf structure. Deep-Sea Research II 53, 2931–2955.

Sanchez, R. F., Relvas, P., Martinho, A., Miller, P., 2008. Physical description of an upwelling filament west of Cape St. Vincent in late October 2004. Journal of Geophysical Research-Oceans 113, doi:10.1029/2007JC004430.

Shaw, W., Robinson, C.L.K., 1998. Night versus day abundance estimates of zooplankton at two coastal stations in British Columbia, Canada. Marine Ecology Progress Series 175, 143–153.

Smith, S.L., Lane, P., 1991. The jet off Point Arena, California: Its role in aspects of secondary production in the copepod Eucalanus californicus Johnson. Journal of Geophysical Research 96, 14849–14858.

Strub, P.T., Kosro, P.M., Huyer, A., 1991. The nature of the cold filaments in the California Current System. Journal of Geophysical Research 96, 14,743–14,768.

Suchman, C.L., Brodeur, R.D., 2005. Abundance and distribution of large medusae in surface waters of the northern California Current. Deep-Sea Research II 52, 51–72.

Sutor, M., Cowles, T.J., Peterson, W.T., 2005. Acoustic observations of finescale zooplankton distributions in the Oregon upwelling region. Deep-Sea Research II 52, 109–121.

Torres, C.R., Mascarenhas, A.S., Castillo, J.E., 2004. Three-dimensional stratified flow over Alarcon Seamount, Gulf of California entrance. Deep-Sea Research II 51, 647–657.

Tynan, C.T., Ainley, D.G., Barth, J.A., Cowles, T.J., Pierce, S.D., Spear, L.B., 2005. Cetacean distributions relative to ocean processes in the northern California Current System. Deep-Sea Research II 52, 145–167.

Uye, S., 1982. Length–weight relationships of important zooplankton from the inland Sea of Japan. Journal of the Oceanographic Society of Japan 38, 149–158.

van Geen, A., Takesue, R.K., Goddard, J., Takahashi, T., Barth, J.A., Smith, R.L., 2000. Carbon and nutrient dynamics during coastal upwelling off Cape Blanco, Oregon. Deep-Sea Research II 47, 975–1002.

Vidal, J., 1980. Physioecology of zooplankton. I. Effects of phytoplankton concentration, temperature, and body size on the growth rate of *Calanus pacificus* and *Pseudocalanus* sp. Marine Biology 56, 111–134.

Wing, S.R., Botsford, L.W., Ralston, S.V., Largier, J.L., 1998. Meroplanktonic distribution and circulation in a coastal retention zone of the Northern California upwelling system. Limnology and Oceanography 43, 1710–1721.

Wishart, D., 1969. An algorithm for hierarchical classifications. Biometrics 25, 165–170.

Wroblewski, J.S., 1982. Interaction of currents and vertical migration in maintaining *Calanus marshallae* in the Oregon upwelling zone—a simulation. Deep-Sea Research 29, 665–686.

Yebra, L., Hernández-León, S., Almeida, C., Bécognée, P., Rodríguez, J.M., 2004. The effect of upwelling filaments and island-induced eddies on indices of feeding, respiration and growth in copepods. Progress in Oceanography 62, 151–169.

Yen, P.P.W., Sydeman, W.J., Bograd, S.J., Hyrenbach, K.D., 2006. Spring-time distributions of migratory marine birds in the southern California Current: oceanic eddy associations and coastal habitat hotspots over 17 years. Deep-Sea Research II 53, 399–418.

Zhou, M., Zhu, Y., 2002. Mesoscale zooplankton distribution and its correlation with physical and fluorescence fields in the California Current in 2000. EOS Transactions American Geophysical Union 83, Abstract OS21N-04.